

Stabilized rapid oscillations in a delay equation: Feedback control by a small resonant delay

– Dedicated to Jürgen Scheurle in gratitude and friendship –

Bernold Fiedler*
Isabelle Schneider*

version of August 27, 2017

*

Institut für Mathematik
Freie Universität Berlin
Arnimallee 3/7
14195 Berlin, Germany

Abstract

We study scalar delay equations

$$\dot{x}(t) = \lambda f(x(t-1)) + b^{-1}(x(t) + x(t-p/2))$$

with odd nonlinearity f , real nonzero parameters λ, b , and two positive time delays $1, p/2$. We assume supercritical Hopf bifurcation from $x \equiv 0$ in the well-understood single-delay case $b = \infty$. Normalizing $f'(0) = 1$, branches of constant minimal period $p_k = 2\pi/\omega_k$ are known to bifurcate from eigenvalues $i\omega_k = i(k + \frac{1}{2})\pi$ at $\lambda_k = (-1)^{k+1}\omega_k$, for any nonnegative integer k . The unstable dimension of these rapidly oscillating periodic solutions is k , at the local branch k . We obtain stabilization of such branches, for arbitrarily large unstable dimension k , and for delicately narrow regions of control amplitudes $b < 0$.

For $p = p_k$ the branch k of constant period p_k persists as a solution, for any $b \neq 0$. Indeed the delayed feedback term controlled by b vanishes on branch k : the feedback control is noninvasive there. Following an idea of [Pyr92], we seek parameter regions $\mathcal{P} = (\underline{b}_k, \bar{b}_k)$ of controls $b \neq 0$ such that the branch k becomes stable, locally at Hopf bifurcation. We determine rigorous expansions for \mathcal{P} in the limit of large k . Our analysis is based on a *2-scale covering lift* for the slow and rapid frequencies involved.

These results complement earlier results by [FiOl16] which required control terms

$$b^{-1}(x(t-\vartheta) + x(t-\vartheta-p/2))$$

with a third delay ϑ near 1.

Contents

1	Introduction and main result	1
2	The 2-scale characteristic equation	9
3	Control-induced Hopf bifurcation	21
4	Locally uniform expansions in $\varepsilon = 1/\omega_k$	34
5	Asymptotic expansions for large $\Omega_m = 1/\delta$	38
6	Proof of theorem 1.2	43

1 Introduction and main result

In an ODE setting, *delayed feedback control* is frequently studied in systems like

$$(1.1) \quad \dot{\mathbf{x}}(t) = \mathbf{F}(\mathbf{x}(t)) + \beta(\mathbf{x}(t) - \mathbf{x}(t - \tau))$$

with $\mathbf{x} \in \mathbb{R}^N$, smooth nonlinearities \mathbf{F} , and suitable $N \times N$ matrices β mediating the feedback. If the uncontrolled system $\beta = 0$ possesses a periodic orbit $\mathbf{x}_*(t)$ of (not necessarily minimal) period $p > 0$, then $\mathbf{x}_*(t)$ remains a solution of (1.1) for time delays $\tau = p$ and any control matrix β . In this sense, the delayed feedback control is noninvasive on $\mathbf{x}_*(t)$. The linearized and nonlinear stability or instability of $\mathbf{x}_*(t)$, however, may well be affected by the control term β .

The above idea was first proposed by Pyragas, see [Pyr92]. It has gained significant popularity in the applied literature since then, with currently around 3000 publications listed. See [Fie&al08] and [Pyr12] for more recent surveys. In fact, no previous knowledge of the nonlinearity \mathbf{F} is required to attempt this procedure, or one of its many variants.

One fundamental disadvantage of the Pyragas method (1.1), from a theoretical perspective, is the replacement of the ODE $\dot{\mathbf{x}} = \mathbf{F}(\mathbf{x})$ in finite-dimensional phase space $X = \mathbb{R}^N$ by the infinite-dimensional dynamical system (1.1) in a history phase space like $\mathbf{x}(t + \cdot) \in X = C^0([-\tau, 0], \mathbb{R}^N)$. On the other hand, the very existence of a periodic solution $\mathbf{x}(t)$, for vanishing control $\beta = 0$, requires $N = 2$.

In [FiOl16] we therefore started to explore the Pyragas method of delayed feedback control, in a slightly modified form, for the very simplistic scalar case

$$(1.2) \quad \dot{x}(t) = \lambda f(x(t - 1)) + b^{-1}(x(t - \vartheta) + x(t - \vartheta - p/2)).$$

We consider nonzero real parameters λ , b and positive delays ϑ , $p/2$. The case $b = 0$ will only appear as a formal limit $\beta = \pm\infty$ of infinite feedback amplitudes. The identical cases $b = \pm\infty$ account for vanishing feedback $\beta = 0$ and correspond to the scalar pure delay equation

$$(1.3) \quad \dot{x}(t) = \lambda f(x(t - 1))$$

with $|\lambda|$ normalizing the remaining delay to unity. Throughout the paper we assume $f \in C^3$ to be odd, with normalized derivative at $f(0) = 0$:

$$(1.4) \quad f(-x) = -f(x), \quad f'(0) = 1, \quad f'''(0) < 0.$$

The characteristic equation for eigenvalues μ of the linearization of (1.2) at parameter λ and the trivial equilibrium $x \equiv 0$ then reads

$$(1.5) \quad \mu = \lambda e^{-\mu} + b^{-1}(e^{-\vartheta\mu} + e^{-(\vartheta+p/2)\mu}).$$

See [KapYor74] for an analysis of odd periodic solutions $x_k(t)$ of (1.3) with constant minimal period

$$(1.6) \quad p_k := 2\pi/\omega_k, \quad \omega_k := (k + \tfrac{1}{2})\pi.$$

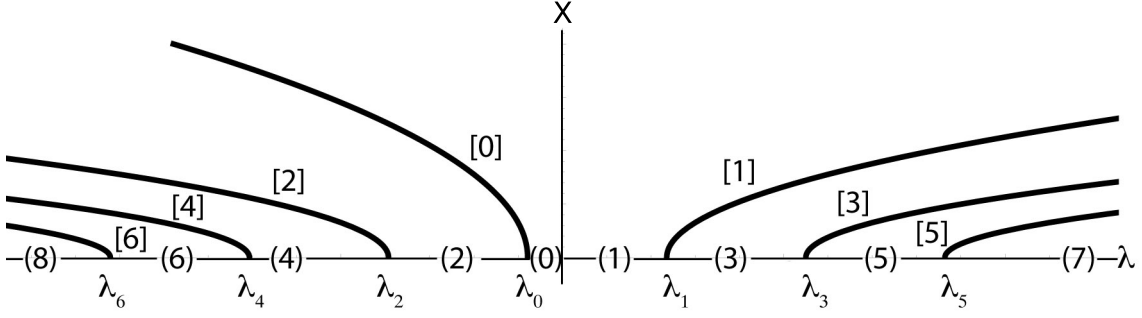


Figure 1.1: Supercritical Hopf bifurcations of (1.3) at $\lambda = \lambda_k$. Note the strict unstable dimensions $E(\lambda_k) = k$ of the trivial equilibrium, in parentheses (k) , and the inherited unstable dimensions $[k]$ of the local branches of bifurcating periodic orbits with constant minimal period $p_k = 4/(2k+1)$. All branches consist of unstable rapidly oscillating periodic solutions, except for the stable slowly oscillating branch $k = 0$. See [FiOl16].

The periodic solutions originate by Hopf bifurcation from imaginary eigenvalues $\pm i\omega_k$ at $x = 0$ for parameters

$$(1.7) \quad \lambda = \lambda_k := (-1)^{k+1} \omega_k.$$

Here $k \in \mathbb{N}_0$ is any nonnegative integer. For $k > 0$, these periodic solutions are called *rapidly oscillating* because their minimal period p_k is at most $4/3$. *Slowly oscillating* periodic solutions, in contrast, have minimal periods exceeding 2. For example, $p_0 = 4$. See [Dor89] for secondary bifurcations from these primary branches. The case $\dot{x}(t) = g(x(t), x(t-1))$ of the general scalar delay equation with a single time lag has also attracted considerable attention; see for example [Wri55, BeCo63, Hale77, HaleVL93, Die&al95, Wu96, KolMysh99, Nu02] and the many references there. Most notably, Mallet-Paret has discovered a discrete Lyapunov functional for g with monotone delayed feedback, [MP88], with significant global consequences [FieMP89, Kri08, Lop17, MPSe96a, MPSe96b, Wal95]. For example, all rapidly oscillating periodic solutions are known to be unstable. More recent developments study this scalar equation with state dependent delays, where the time delay 1 is not constant but depends on the history $x(t + \cdot)$ of the solution itself; see for example [Har&al06, MPNu92, MPNu96, MPNu03, MPNu11, Nu02].

But let us return to the simple setting (1.3)–(1.6) of a pure delay equation. Pioneering analysis by [KapYor74] reduces the quest for periodic solutions near all Hopf bifurcations (1.7) to a planar Hamiltonian ODE system. This is due to an *odd-symmetry*

$$(1.8) \quad x_k(t + p_k/2) = -x_k(t)$$

at half minimal period p_k , for all real t . See also [FiOl16] for complete details, and [YuGuo14] for a survey on the Kaplan-Yorke idea. Remarkably, global solution branches of constant minimal period p_k emanate from each $\lambda = \lambda_k$ towards λ of larger absolute value, in the soft spring case of strictly decreasing secant slopes $x \mapsto f(x)/x$, for $x > 0$. In particular all Hopf bifurcations are locally nondegenerate

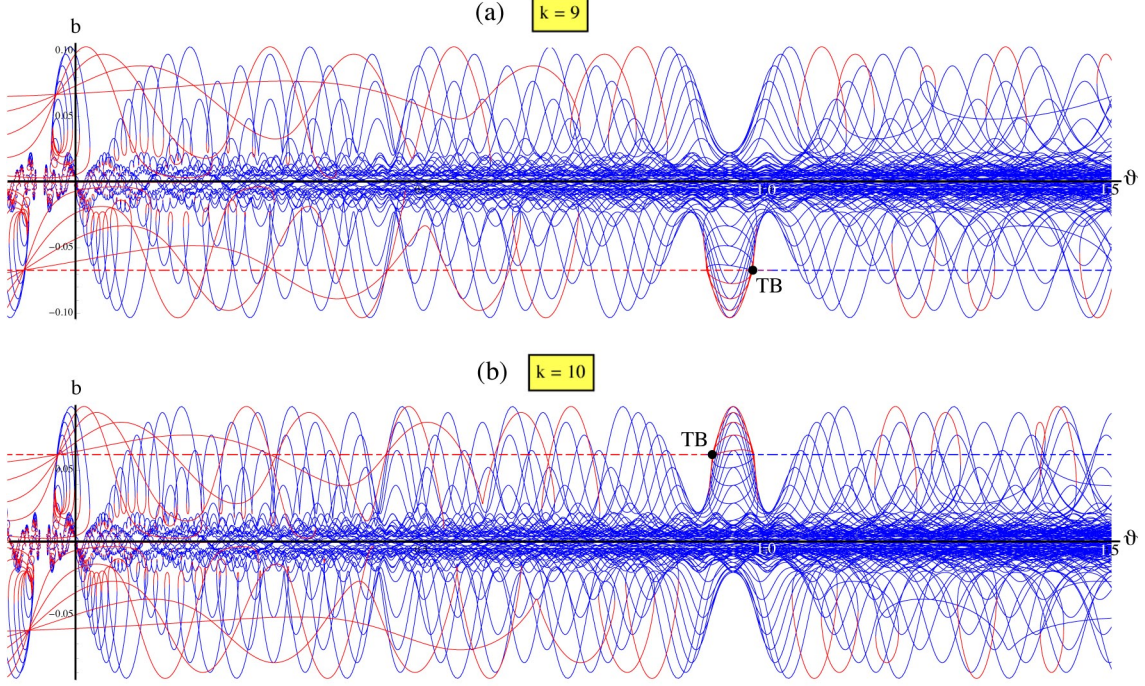


Figure 1.2: Additional Hopf curves (colored solid), zero eigenvalue (colored dashed), and Takens-Bogdanov bifurcations (TB, black) at fixed $\lambda = \lambda_k$, for odd $k = 9$, (a) top, and even $k = 10$, (b) bottom. The Hopf curves are generated by the control parameters ϑ and b of the delayed feedback terms in (1.2). The more stable side is found towards smaller $|b|$, at red Hopf branches, and towards larger $|b|$, at blue branches. The same statement holds true at the zero eigenvalue; see the red dashed line. See [FiOl16] for further details.

and quadratically supercritical under the sign assumption $f'''(0) < 0$ of (1.4). See fig. 1.1 for a bifurcation diagram.

At supercritical Hopf bifurcation it is easy to determine the unstable dimension E , i.e. the total algebraic multiplicity of Floquet multipliers outside the complex unit circle, for the emanating local branch of periodic orbits. It coincides with the total algebraic multiplicity

$$(1.9) \quad E = E(\lambda_k) = k$$

of the eigenvalues with strictly positive real part for the linearization of the pure delay equation (1.3) at the Hopf point $\lambda = \lambda_k$, $x \equiv 0$. See for example [Die&al95, Hale77, HaleVL93]. Henceforth we skip trivial case $k = 0$, which leads to the bifurcation of stable, slowly oscillating solutions. Let $k \in \mathbb{N}$ be any strictly positive integer.

The local (and global) Hopf branches $(\lambda, x_k(t))$ which bifurcate at $\lambda = \lambda_k$, $x = 0$ inherit constant period $p = p_k$ and odd-symmetry (1.8). Therefore our modified Pyragas control scheme (1.2) with $p := p_k$ is noninvasive on the Hopf branches with this symmetry. For earlier applications of Pyragas control at half minimal periods in the presence of some symmetry, although not in our delay context, we refer to

[NakUe98, Fie&al10]. It is our main objective to stabilize all bifurcating periodic orbits, for any unstable dimension $k \in \mathbb{N}$, by suitable Pyragas controls (1.2). For odd k , this again refutes the purported “odd number limitation” of Pyragas control [Fie&al07, Ju&al07, Nak97, NakUe98].

We define a *Pyragas region* \mathcal{P} to be a connected component of real control parameters $b \neq 0$ and $\vartheta \geq 0$ for which the periodic solutions $x_k(t)$ emanating by local Hopf bifurcation from $\lambda = \lambda_k$, $x \equiv 0$ become linearly asymptotically stable for sufficiently small amplitudes. Therefore, the boundaries of Pyragas regions are either certain curves where zero eigenvalues $\mu = 0$ occur, or else are Hopf curves characterized by purely imaginary eigenvalues $\mu = i\tilde{\omega}$ of the characteristic equation (1.5). With this definition we can now formulate the main result of [FiOl16]. See fig. 1.2 for an illustration of Hopf curves in the cases $k = 9$ and $k = 10$.

Theorem 1.1. [FiOl16] *Consider the system (1.2) of delayed feedback control for the scalar pure delay equation (1.3). Let assumptions (1.4) of oddness and normalization hold for the soft spring nonlinearity $f \in C^3$. Then the following assertions hold for large enough $k \geq k_0$.*

There exist Pyragas regions $\mathcal{P} = \mathcal{P}_k^+ \cup \mathcal{P}_k^-$ composed of two disjoint open sets $\mathcal{P}_k^\pm \neq \emptyset$. Each region \mathcal{P}_k^ι , $\iota = \pm$, is bounded by the horizontal zero line

$$(1.10) \quad b = b_k := -2/\lambda_k = (-1)^k \cdot 2/\omega_k$$

and three other analytic curves γ_k^0 and $\gamma_{k,\pm}^\iota$, all mutually transverse. The zero line (1.10) indicates an additional zero eigenvalue of the linearization of (1.2) at $x \equiv 0$. The other curves indicate additional purely imaginary eigenvalues.

Define $\varepsilon := 1/\omega_k$. Then an approximation of the Pyragas regions $(\vartheta, b) \in \mathcal{P}_k^\iota$, $\iota = \pm$, up to error terms of order ε^3 , is given by two parallelograms. One exact horizontal boundary is $b = b_k := (-1)^k 2\varepsilon$; see (1.10). The other horizontal boundary γ_k^0 is approximated by

$$(1.11) \quad b = (-1)^k 2\varepsilon + b_k^\iota \varepsilon^2 + \dots$$

The sides $\gamma_{k,\pm}^\iota$ are given, up to order ε^3 , by the parallel slanted lines through the four points at $b = b_k$,

$$(1.12) \quad \vartheta_{k,\pm}^\iota = 1 - (\tfrac{\pi}{2} - \iota q) \varepsilon \pm \Theta_{k+2} \varepsilon^2 + \dots,$$

with slopes σ_k^ι . The offsets q , Θ_{k+2} , b_k^ι and the slopes σ_k^ι of the Pyragas parallelograms are given by

$$(1.13) \quad \begin{aligned} q &= \arccos(2/\pi) &= 0.88\dots, \\ \Theta_{k+2} &= \pi(\sqrt{(\pi/2)^2 - 1} - 2q) &= -1.73\dots, \\ b_k^\iota &= (\pi + 2\Phi_k^\iota) \cos \Phi_k^\iota &= 1.49\dots + (-1)^k \iota \cdot 1.02\dots, \\ \sigma_k^\iota &= 2(-1)^{k+1} \iota \sqrt{(\pi/2)^2 - 1} &= (-1)^{k+1} \iota \cdot 2.42\dots \end{aligned}$$

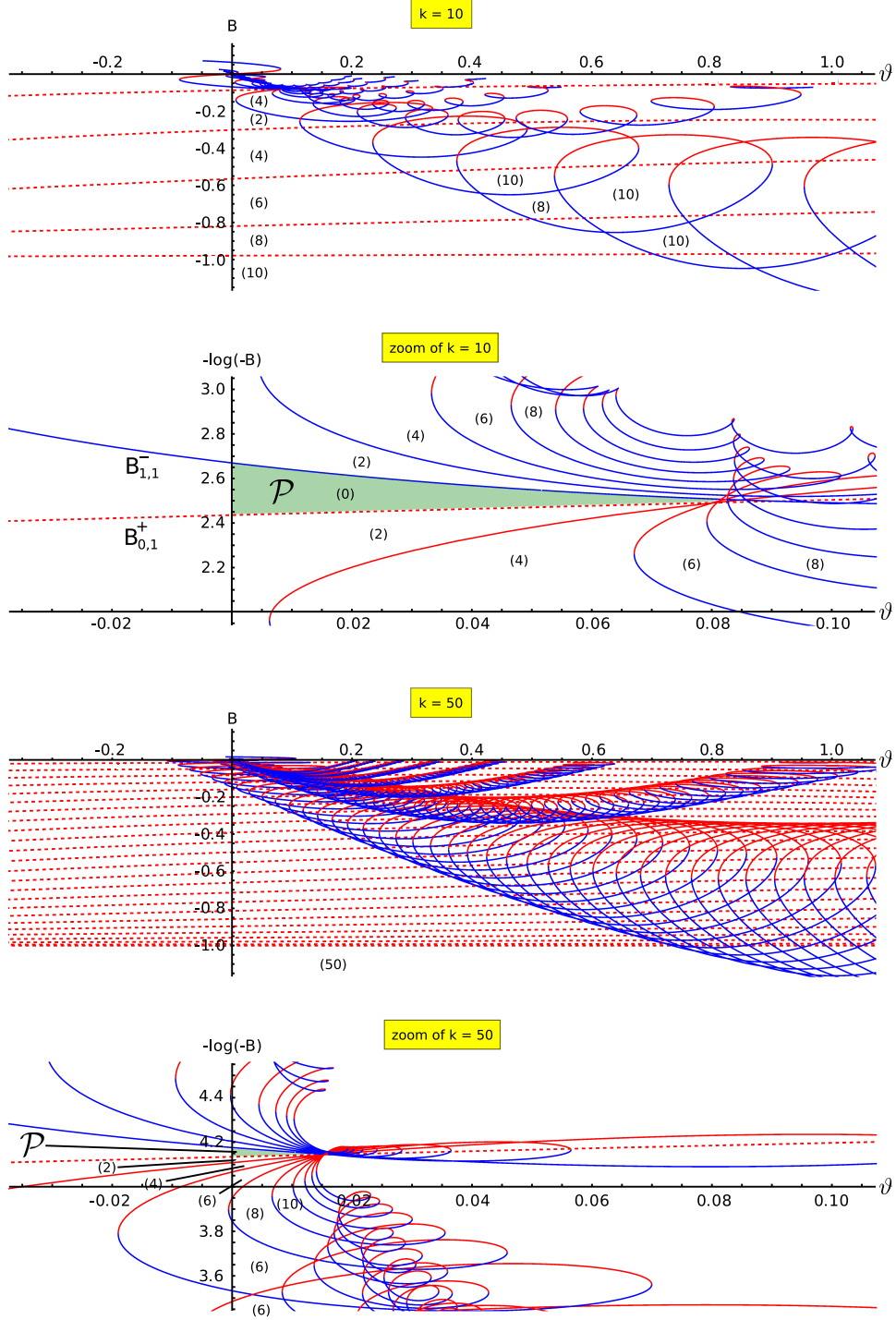


Figure 1.3: Control induced Hopf curves in parameters (ϑ, b) , as in fig 1.2, near $\vartheta = 0$. (a) $k = 10$, (b) zoom into $k = 10$, (c) $k = 50$, (d) zoom into $k = 50$. Vertical coordinates are B , in (a), (c), and $-\log(-B)$, for the zooms (b),(d), with scaled $B = \frac{1}{2}b\omega_k$. Pyragas regions \mathcal{P} are indicated in green. Hopf curves $\mu = i\tilde{\omega}$ with Hopf frequencies $0 < \tilde{\omega} < \omega_k$ are dashed (red), and Hopf curves with $\tilde{\omega} > \omega_k$ are solid (red, blue). For color coding see fig 1.2. Unstable dimensions $E(b, \vartheta)$ of $x \equiv 0$, and of bifurcating periodic orbits, are indicated in parentheses.

Here we have used the abbreviations

$$(1.14) \quad \Phi_k^\iota = (-1)^k \iota \arcsin q.$$

In particular the areas $|\mathcal{P}_k^\pm|$ of the Pyragas regions are of very small order ε^4 . The relative areas are approximately reciprocal,

$$(1.15) \quad \lim_{k \rightarrow \infty} |\mathcal{P}_k^+|/|\mathcal{P}_k^-| = b_k^+/b_k^- = \begin{cases} 5.37 \dots & \text{for even } k, \\ 0.19 \dots & \text{for odd } k. \end{cases}$$

See [FiOl16] for full details and proofs.

The above stabilization result for rapidly oscillating periodic solutions requires two additional delays in the control term of (1.2): the half-period delay $p_k/2$, and a joint offset ϑ near 1, in addition to the normalized delay 1 of the reference system. In the present paper we achieve the same goal with the single delay $p_k/2$ in the control term, i.e. with delay offset:

$$(1.16) \quad \vartheta = 0.$$

From now on, and for the rest of the paper, we therefore replace (1.2) by

$$(1.17) \quad \dot{x}(t) = \lambda f(x(t-1)) + b^{-1}(x(t) + x(t-p/2)),$$

with nonlinearities $f \in C^3$ which satisfy assumptions (1.6). Our main result identifies unique nonempty Pyragas intervals $\mathcal{P}_k = (\underline{b}_k, \bar{b}_k)$ of control parameters b . The k -dimensionally unstable, rapidly oscillating periodic solutions of constant minimal period $p_k = 4/(2k+1)$ are stabilized near Hopf bifurcation at $\lambda = \lambda_k$, $x = 0$, for $b \in \mathcal{P}_k$ and arbitrarily large $k \in \mathbb{N}$. Via $\varepsilon := 1/\omega_k = p_k/2\pi$, we also provide ε -expansions, alias k -expansions, for the Pyragas boundaries \underline{b}_k and \bar{b}_k .

Theorem 1.2. *Consider the system (1.17) of delayed feedback control for the scalar pure delay equation (1.3). Let assumptions (1.4) of oddness and normalization hold for the soft spring nonlinearity $f \in C^3$. Then the following assertions hold for large enough $k \geq k_0$, i.e. for small enough $0 < \varepsilon := 1/\omega_k = ((k+1/2)\pi)^{-1} \leq \varepsilon_0$.*

The only Pyragas region of nonzero control amplitudes b is the open interval

$$(1.18) \quad \mathcal{P}_k := \{\underline{b}_k < b < \bar{b}_k\}.$$

Up to error terms of order ε^4 , the lower and upper bounds of the Pyragas interval satisfy

$$(1.19) \quad \begin{aligned} \underline{b}_k &= -\frac{1}{2}\pi^2\varepsilon^2 - \frac{3}{4}\pi^3\varepsilon^3 + \dots, \\ \bar{b}_k &= -\frac{1}{2}\pi^2\varepsilon^2 + \frac{1}{4}\pi^3\varepsilon^3 + \dots. \end{aligned}$$

Although our proofs and expansions only address Hopf bifurcations at sufficiently large unstable dimensions k , and sufficiently rapid oscillation frequencies ω_k , numerical evidence suggests a single Pyragas interval \mathcal{P}_k , for any $k \geq 1$. We do not pursue these cases here, beyond the evidence in figs. 1.2 and 1.3.

The remaining sections contribute to the proof of theorem 1.2. We give a brief outline here. For a summary of sections 2–5, on a precise technical level, we also recommend the proof of theorem 1.2 in the concluding section 6.

Section 2 and most of the remaining sections address the characteristic equation for the linearization at the original Hopf bifurcation points $\lambda = \lambda_k$, $x \equiv 0$. In section 2 we recall some elementary results from [FiOl16] which address the crossing direction of an additional simple eigenvalue 0 induced by the control term. We introduce a *2-scale lift*, which artificially represents the large imaginary parts of b -induced Hopf eigenvalues $\mu = i\tilde{\omega}$ by, both, $\tilde{\omega}$ itself and a scaled slow frequency

$$(1.20) \quad \tilde{\Omega} = \varepsilon \tilde{\omega}.$$

Note how $\tilde{\Omega} = 1$, $\tilde{\omega} = \omega_k$ correspond to the reference Hopf bifurcation at $\lambda = \lambda_k$. We observe $\tilde{\Omega} \neq 2m$ cannot be at even integer resonance. We introduce a new local scaled slow frequency

$$(1.21) \quad \Omega := \tilde{\Omega} - \Omega_m, \quad \Omega_m := 2m + 1,$$

near each odd integer resonance Ω_m . Below, in fact, we will be able to focus on $-1 < \Omega \leq 0$. Since

$$(1.22) \quad \omega \equiv \tilde{\omega} \pmod{2\pi}$$

rotates rapidly through S^1 , for small ε , we treat the two frequencies Ω, ω as independent variables, formally. They remain related by the *hashing relation*

$$(1.23) \quad \Omega = \varepsilon(\omega + \frac{\pi}{2}(1 - (-1)^k - (-1)^m) - 2\pi j), \quad -\frac{\pi}{2} \leq \omega < \frac{3}{2}\pi,$$

$j \in \mathbb{N}$, first discussed in lemma 2.3. We will be able to restrict attention to the case of odd k , in this setting.

For the control amplitude b we consider the same scaling

$$(1.24) \quad B := \frac{1}{2}b\varepsilon^{-1}$$

as in [FiOl16]. We thus arrive at the *2-scaled characteristic equation*

$$(1.25) \quad 0 = -ie^{i\omega} + \Omega_m + \Omega + (-1)^m B^{-1} \cos(\frac{\pi}{2}\Omega) e^{i\frac{\pi}{2}\Omega}.$$

In lemmata 2.4–2.6 we solve the ε -independent (!) complex characteristic equation (1.25) for the real variables

$$(1.26) \quad \begin{aligned} \omega &= \omega^\pm(\Omega) \\ B &= B^\pm(\Omega). \end{aligned}$$

See figs. 2.1, 2.2 for illustration.

In section 3 we observe how the imaginary parts $\tilde{\omega}$ of unstable eigenvalues $\mu = \mu_R + i\tilde{\omega}$ are trapped in certain strips indexed by m, j . Instability in such a strip can be induced by Hopf bifurcation at control parameters $B = B_{m,j}^-$, and be reduced again at control parameters $B_{m,j}^+$. This involves an analysis of the crossing directions of μ , transversely to the imaginary axis $\mu_R = 0$, as B increases through $B_{m,j}^\pm$. See fig. 3.1 and theorem 3.4. In corollary 3.6 we conclude the absence of any region of Pyragas stabilization for $B > 0$. Corollary 3.9 summarizes the results of section 3: we reduce the proof of theorem 1.2 to three inequalities among the Hopf values $B_{m,j}^\pm$; see (3.77), (3.78), and (3.79).

In section 4, we insert the solution $\omega = \omega^\pm(\Omega)$ from (1.26) into the hashing (1.23). Inverting the resulting maps $\Omega \mapsto \varepsilon = \varepsilon(\Omega)$, uniformly for bounded $m \leq m_0$, $j \leq j_0$, we obtain ε -expansions

$$(1.27) \quad \begin{aligned} \Omega &= \Omega_{m,j}^\pm(\varepsilon) \\ \omega &= \omega_{m,j}^\pm(\varepsilon) \\ B &= B_{m,j}^\pm(\varepsilon) \end{aligned}$$

for the frequencies $\tilde{\omega} \equiv \omega$ and the control amplitudes $b = 2B\varepsilon$ of the resulting control-induced Hopf bifurcations. In particular the crossing directions of the induced imaginary Hopf pairs with respect to b sum up such that

$$(1.28) \quad \underline{b} = 2\varepsilon B_{0,1}^+(\varepsilon), \quad \bar{b} = 2\varepsilon B_{1,1}^-(\varepsilon)$$

provide the boundaries of the Pyragas region \mathcal{P} claimed in theorem 1.2. We illustrate the relative location of $B_{m,j}^\pm$, in view of the crucial inequalities required in corollary 3.9, at the end of section 4; see also fig 4.1.

It remains to show, however, that the candidate interval $b \in (\underline{b}, \bar{b})$ does not suffer any destabilization, due to any other Hopf points $B_{m,j}^\pm$. This turns out to be equivalent to the estimates

$$(1.29) \quad B_{m,j_m+1}^+ < B_{0,1}^+ \quad \text{and} \quad B_{m,j_m}^- > B_{1,1}^-$$

at $j_m := [(m+1)/2]$. See (3.77), (3.79) and corollary 3.9 again. For bounded $m \leq m_0$, these estimates are suggested by the explicit expansions (1.27). In section 5 we begin to settle the delicate case of large m, Ω_m by expansions with respect to

$$(1.30) \quad \delta := \Omega_m^{-1} = 1/(2m+1).$$

Here our second small parameter $\delta > 0$ expands the odd integer resonance regions around $\Omega = \Omega_m = 2m+1$, for large m , in much the same way as our first small parameter ε expanded the discrete parameter k , for large $k \geq k_0$, which enumerated the original Hopf bifurcations of more and more rapidly oscillating periodic solutions with higher and higher unstable dimension.

Again we solve the characteristic equation (1.25) to obtain expansions

$$(1.31) \quad \begin{aligned} \Omega &= \Omega^\pm(\delta, \omega), \\ B &= B^\pm(\delta, \omega) \end{aligned}$$

with respect to δ , uniformly in $|\omega| \leq \pi/2$. This time, Ω^-, B^- refer to the case $j = j_m$ and Ω^+, B^+ refer to $j = j_m + 1$. In section 5, the hashing relation (1.23) then provides a δ -expansion for

$$(1.32) \quad \varepsilon^\pm = \varepsilon^\pm(\delta, \omega).$$

Inserting this into the already established expansions (1.28) for \underline{b}, \bar{b} , and comparing the results, for small δ , we obtain

$$(1.33) \quad B^+(\delta, \omega) < B_{0,1}^+(\varepsilon^+(\delta, \omega)) \quad \text{and} \quad B^-(\delta, \omega) > B_{1,1}^-(\varepsilon^-(\delta, \omega))$$

as claimed in (1.29). Well, nontrivial differences only appear at order δ^3 and after additional linearization with respect to ω , at $\omega = \pm\pi/2$.

The proof of theorem 1.2 only involves some discussion of a characteristic equation with two exponential terms of different scales. Nevertheless, the elementary ingredients to the proof turned out to be surprisingly involved. Therefore we summarize the various elements of the proof, as scattered across sections 2–5, in our final section 6.

Acknowledgments. For many helpful comments and suggestions, as well as most of the figures, we are much indebted to Alejandro López Nieto. Ulrike Geiger cheerfully converted yet another manuscript into the present form, with all her expertise and singular diligence. The authors have been supported by the CRC 910 “*Control of Self-Organizing Nonlinear Systems: Theoretical Methods and Concepts of Application*” of the Deutsche Forschungsgemeinschaft.

2 The 2-scale characteristic equation

The characteristic equation (1.5) of the delay equation (1.2) with vanishing time shift $\vartheta = 0$ reads

$$(2.1) \quad \mu = -(1)^k \varepsilon^{-1} e^{-\mu} + b^{-1} (1 + e^{-\pi \varepsilon \mu}),$$

at Hopf bifurcation parameter $\lambda = \lambda_k = (-1)^{k+1} \omega_k$, and with the abbreviation

$$(2.2) \quad \varepsilon = \omega_k^{-1} = 1/((k + \frac{1}{2})\pi)$$

for $k \in \mathbb{N}$. We decompose the eigenvalue $\mu = \mu_R + i\tilde{\omega}$ into real and imaginary parts and define the auxiliary slow frequency $\tilde{\Omega} := \varepsilon \tilde{\omega}$; see (1.20). For the convenient choice of

$$(2.3) \quad \omega := \tilde{\omega} \pmod{2\pi}, \quad -\frac{1}{2}\pi \leq \omega < \frac{3}{2}\pi,$$

we obtain the crucially important 2-scale characteristic equation

$$(2.4) \quad \begin{aligned} 0 &= \chi(\varepsilon, \delta, \omega, \Omega, B, \mu_R) := \\ &= -\varepsilon\mu_R + i\tilde{\Omega} - (-1)^k e^{-\mu_R + i\omega} - \frac{i}{B} \sin\left(\frac{\pi}{2}\Omega\right) e^{-\pi\varepsilon\mu_R + i\frac{\pi}{2}\Omega} + \frac{1}{2B}(1 - e^{-\pi\varepsilon\mu_R}), \end{aligned}$$

by some elementary arithmetic and with the abbreviations

$$(2.5) \quad \begin{aligned} \tilde{\Omega} &:= \varepsilon\tilde{\omega}; \\ B &:= \frac{1}{2}b\varepsilon^{-1}; \\ \delta &:= \Omega_m^{-1} = 1/(2m+1); \\ \Omega &:= \tilde{\Omega} - \Omega_m. \end{aligned}$$

Here we recall that $\tilde{\Omega} = 1$ indicates $\tilde{\omega} = \omega_k$, i.e. a $1 : 1$ resonance $\tilde{\omega} = \omega_k$ of the imaginary part $i\tilde{\omega}$ of μ , under feedback control, with the original Hopf eigenvalue $\mu = i\omega_k$ at parameter $\lambda = \lambda_k$. Similarly, $\tilde{\Omega} = \Omega_m = (2m+1)$ indicates an odd integer $(2m+1) : 1$ resonance. The parameters ε, δ make k, m look continuous, respectively, and replace them eventually.

For complex nonreal eigenvalues μ , the imaginary part $\tilde{\omega} = \tilde{\Omega}/\varepsilon$ can be taken positive, without loss, and we may assume

$$(2.6) \quad \begin{aligned} -1 &< \Omega \leq 0, & \text{for } m = 0, \\ -2 &< \Omega \leq 0, & \text{for } m \in \mathbb{N}. \end{aligned}$$

We also note that χ is real analytic in all variables, for $B \neq 0$. Since $\mu_R = 0$, for purely imaginary eigenvalues, the characteristic function χ of (2.4) simplifies and becomes

$$(2.7) \quad \chi_0(\delta, \omega, \Omega, B) := -i\chi(\varepsilon, \delta, \omega, \Omega, \mu_R = 0) = \tilde{\Omega} + (-1)^k i e^{i\omega} - \frac{1}{B} \sin\left(\frac{\pi}{2}\Omega\right) e^{i\frac{\pi}{2}\Omega},$$

in the Hopf case. Note how ε has disappeared from the characteristic equation (2.4), in (2.7), at the price of a hidden hashing relation between ω and Ω ; see lemma 2.3 below. Evidently, the solutions of (2.4) for even parity of k are trivially obtained from the solutions for odd parity if we replace ω by $\omega + \pi \pmod{2\pi}$.

In the present section we collect some elementary facts about the 2-scale characteristic equation (2.4)–(2.5). Real eigenvalues $\mu = \mu_R$, i.e. the case $\tilde{\omega} = \tilde{\Omega} = 0$, are addressed in lemma 2.1. As a corollary we eventually obtain how B has to be negative in any Pyragas region; see corollaries 2.2 and 3.6. With a brief interlude on hashing in lemma 2.3, we embark on our discussion of purely imaginary eigenvalues $\mu_R = 0$. In lemma 2.4 we show how to eliminate any two of the three variables ω, Ω, B from the resulting ε -independent 2-scale characteristic equation

$$(2.8) \quad 0 = \chi_0(\delta, \omega, \Omega, B).$$

In particular we identify a quadratic loop

$$(2.9) \quad Q(\delta, \Omega, B) = 0,$$

by elimination of ω , such that purely imaginary eigenvalues $\mu_R = 0$ can occur only if (2.9) is satisfied. In section 3 we will observe how positive real parts, $\mu_R > 0$, can only occur inside the loop, and negative real parts, i.e. linear stability as required in Pyragas regions, are confined to the exterior. Via hashing, this leads to the definition of crucial Hopf values

$$(2.10) \quad B_{m,j}^- < B_{m,j}^+ < 0$$

such that the loss of stability caused at $B_{m,j}^-$, by a pair of purely imaginary eigenvalues, is recovered when the control parameter $B < 0$ increases further to pass the other Hopf value $B_{m,j}^+$.

Lemma 2.1. *The characteristic equation (2.1) possesses a real zero eigenvalue, $\mu = \mu_R = 0$, if and only if*

$$(2.11) \quad B = B_0 = (-1)^k.$$

The zero eigenvalue μ is algebraically simple, and its continuation $\mu = \mu(B)$ satisfies

$$(2.12) \quad \text{sign } \text{Re } \mu'(B_0) = (-1)^k = B_0,$$

i.e. $\mu(B)$ increases towards larger $|B|$.

Proof. For real eigenvalues $\mu = \mu_R$, $\omega = \tilde{\Omega} = 0$, and $\Omega = -1$, the characteristic equation (2.4) reads

$$(2.13) \quad \varepsilon \mu_R = -(-1)^k e^{-\mu_R} + \frac{1}{2B} (1 + e^{-\pi \varepsilon \mu_R}).$$

Inserting $\mu_R = 0$ proves claim (2.11). Partial differentiation with respect to μ_R shows simplicity of $\mu_R = 0$ at $B = B_0 = (-1)^k$. Implicit differentiation with respect to B at $B = B_0$, $\mu_R = 0$ shows

$$(2.14) \quad \begin{aligned} \varepsilon \mu'_R &= (-1)^k \mu'_R + \frac{1}{2} (-1)^k \cdot (-\pi \varepsilon) \mu'_R - 1, \quad \text{i.e.} \\ \mu'_R (1 - (\frac{\pi}{2} + B_0) \varepsilon) &= B_0. \end{aligned}$$

For $k \in \mathbb{N}$, $\varepsilon = 1/((k + 1/2)\pi)$, the coefficient of μ'_R is positive, and the lemma is proved. \boxtimes

Of course we may solve the real characteristic equation (2.13) for $B = B(\mu_R)$, explicitly, to obtain

$$(2.15) \quad B = B(\mu_R) = \frac{1}{2} \cdot \frac{1 + \exp(-\pi \varepsilon \mu_R)}{\varepsilon \mu_R + (-1)^k \exp(-\mu_R)}.$$

For odd k , vanishing denominator indicates the unique positive real eigenvalue $\mu = \mu_R$ of the original problem (1.3) without control. For even k , the denominator is

positive for all real μ_R , because $\varepsilon = (\pi(k + \frac{1}{2}))^{-1} < e$ for $k \in \mathbb{N}$. Moreover, $\pi\varepsilon \leq 2/3$ implies $\lim B(\mu_R) = 0$ for $\mu_R \rightarrow \pm\infty$. Let

$$(2.16) \quad 1 < B_{\max} := \max B(\mu_R) < \infty$$

denote the maximum over $\mu_R \in \mathbb{R}$, for even k . Indeed $B_{\max} > 1 = B_0 = B(0)$, by lemma 2.1. This allows us to determine the parity of the total algebraic count $E(B)$ of all eigenvalues μ , real or complex, with strictly positive real part.

Corollary 2.2. *Let $k \in \mathbb{N}$ be odd. Then the unstable parities (mod 2) are given by*

$$(2.17) \quad E(B) \equiv \begin{cases} 1 & -\infty < B < -1, \\ 0 & \text{for } -1 \leq B < 0, \\ 1 & 0 \leq B < +\infty. \end{cases}$$

For even $k \in \mathbb{N}$, the unstable parities (mod 2) are given by

$$(2.18) \quad E(B) \equiv \begin{cases} 0 & -\infty < B < 0, \\ 1 & \text{for } 0 < B < 1, \\ 0 & 1 \leq B < +\infty. \end{cases}$$

Pyragas regions $E(B) = 0$ require even parity 0 (mod 2), of course. For even k , they also require

$$(2.19) \quad B > B_{\max} > 1,$$

in case $B > 0$.

Proof. Since complex eigenvalues occur in complex conjugate pairs, the real eigenvalues alone determine the parity. For odd k and at $B = \pm\infty$, i.e. at vanishing control, instability by a simple positive real eigenvalue follows from the vanishing denominator in (2.15). Lemma 2.1 then implies claim (2.17).

For even k , real eigenvalues are absent if $B < 0$ or $B > B_{\max}$; see (2.15), (2.16). At $B = B_{\max} > 1$, a pair of complex eigenvalues merges and forms a positive double real eigenvalue. Decreasing B further, one of these two positive eigenvalues becomes negative, at $B = B_0 = 1$, and the other real eigenvalue remains positive and simple; see lemma 2.1. This proves claims (2.18), (2.19), and the corollary. \bowtie

We study the case of purely imaginary nonzero eigenvalues $\mu = i\tilde{\omega} \neq 0$, $\mu_R = 0$ next. The 2-scale characteristic equation (2.4) then simplifies to (2.7), (2.8), i.e.

$$(2.20) \quad \chi_0(\delta, \omega, \Omega, B) := -i\chi(\varepsilon, \delta, \omega, \Omega, B, \mu_R = 0) = 0.$$

Strictly speaking, however, the frequency $\tilde{\omega}$ and the slow frequency $\tilde{\Omega}$ are still related by the linear hashing relation $\tilde{\Omega} = \varepsilon\tilde{\omega}$; see (1.20)–(1.23). We clarify this relation next.

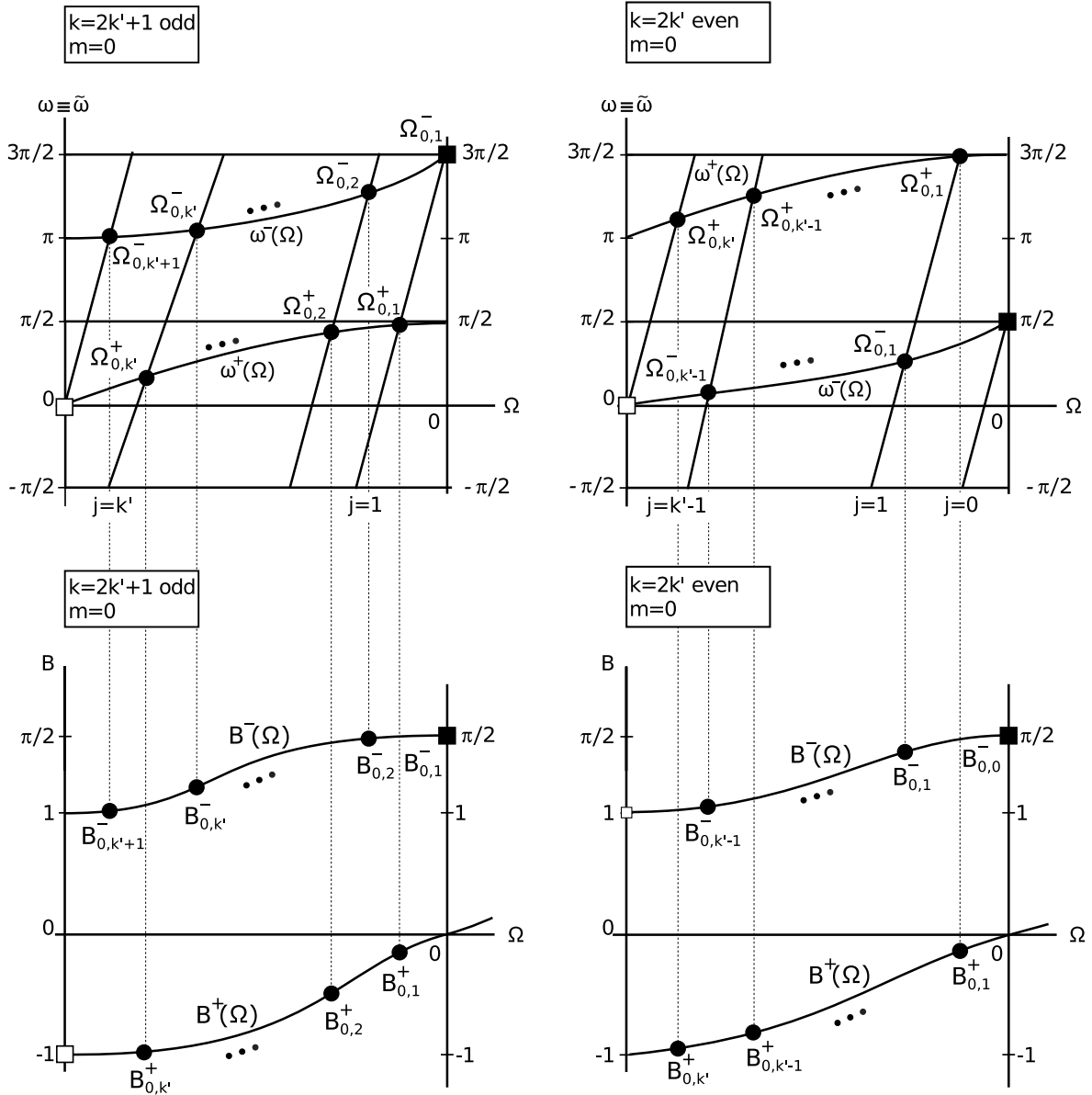


Figure 2.1: Purely imaginary eigenvalues $\mu = i\tilde{\omega} = i\tilde{\omega}_{0,j}^\pm$ and Hopf control parameters $B = B_{0,j}^\pm$ at $\varepsilon = \omega_k^{-1} = ((k + 1/2)\pi)^{-1}$. The horizontal axis is $-1 \leq \Omega = \tilde{\Omega} - \Omega_0 \leq 0$ with $\Omega_0 = 1$. Left: odd k . Right: even k . Top row: hashing $\tilde{\Omega} = \varepsilon\tilde{\omega}$ alias $\Omega = \varepsilon(\omega + \dots)$ according to lemma 2.3, (2.21)–(2.24) and (3.45). Note how $\tilde{\Omega} = \tilde{\Omega}_{0,j}^\pm = \varepsilon\tilde{\omega}_{0,1}^\pm$ enumerate the Hopf frequencies defined by the intersections of the slanted hashing lines, of slope $1/\varepsilon$, with the relations $\tilde{\omega} = \tilde{\omega}^\pm(\tilde{\Omega})$, induced by the 2-scale characteristic equation; see lemma 2.4 and (3.49). Bottom row: the resulting control parameters $B = B_{0,j}^\pm = B^\pm(\tilde{\Omega}_{0,j}^\pm)$, also induced by the 2-scale characteristic equation according to lemma 2.4. Solid dots \bullet indicate transverse Hopf bifurcations, where the Hopf pair $\mu = \pm i\omega$ crosses towards the stable side for decreasing $|B|$, see lemma 2.4(iv). Note the real eigenvalue \square at Hopf frequency $\tilde{\omega} = 0$, for $B = (-1)^k$. Also note the non-crossing trivial Hopf pair \blacksquare at $\mu = \pm i\omega_k$, which terminates the curves $B^-(\tilde{\Omega})$ at $\tilde{\Omega} = \varepsilon\omega_k = 1$.

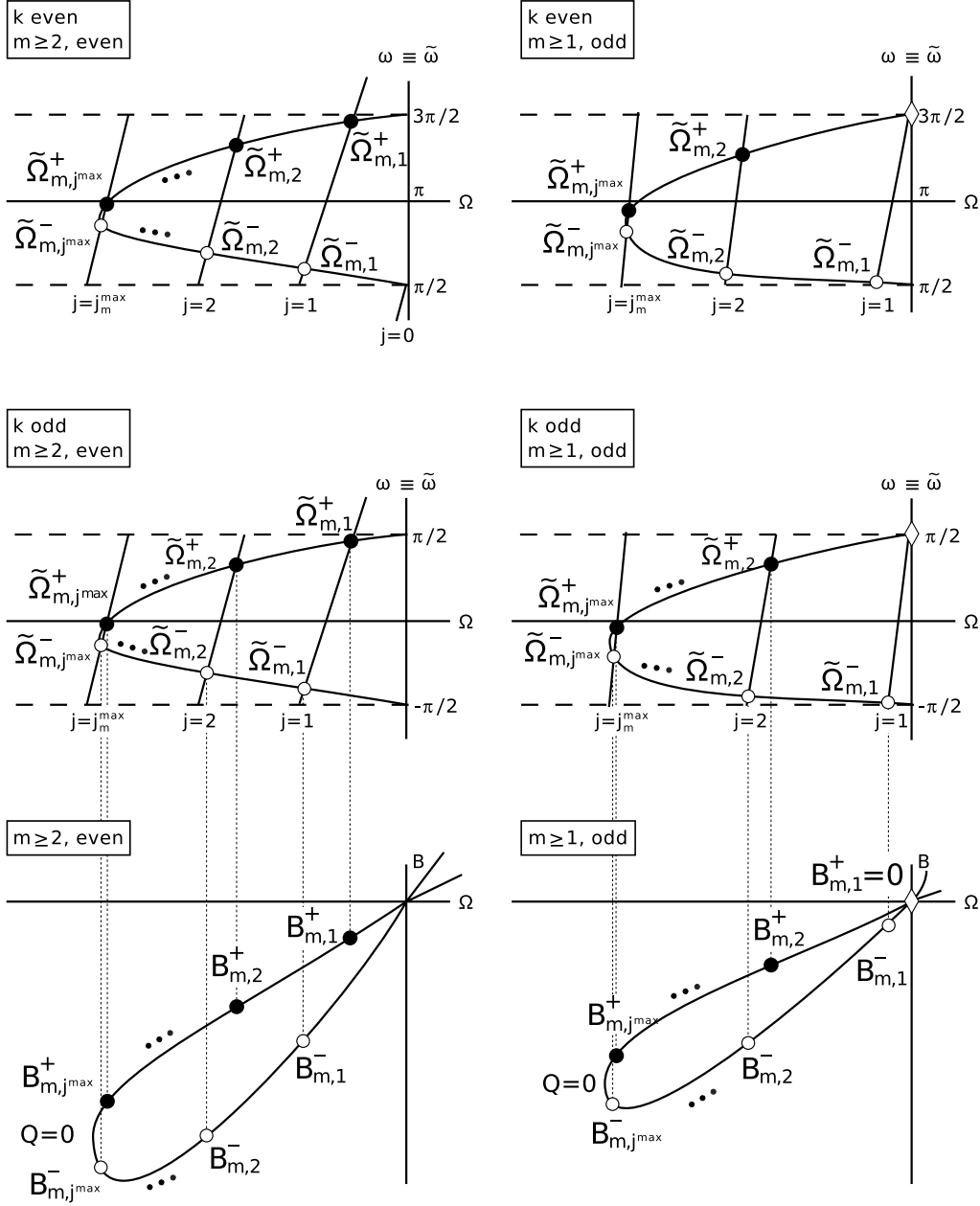


Figure 2.2: Purely imaginary eigenvalues $\mu = i\tilde{\omega} = i\tilde{\omega}_{m,j}^{\pm}$, two top rows, and Hopf control parameters $B = B_{m,j}^{\pm} < 0$, bottom rows, at $\varepsilon = \omega_k^{-1} = ((k + 1/2)\pi)^{-1}$. The horizontal axis is $-1 < \underline{\Omega} \leq \Omega = \tilde{\Omega} - \Omega_m \leq 0$ with $\Omega_m = 2m + 1$. Left: even m . Right: odd m ; for $\Omega_m - 1 < \underline{\Omega}_m \leq \Omega \leq 0$. Layout and legends as in figure 2.1. Again, solid dots \bullet indicate transverse Hopf stabilization towards smaller control parameters $|B|$, i.e. towards larger $B < 0$, at $B_{m,j}^+$. Circles \circ , in contrast, indicate transverse Hopf destabilization towards the same side, at $B_{m,j}^-$. Note how destabilization by each $B_{m,j}^- < 0$ is annihilated when $B < 0$ increases through the subsequent stabilization at $B_{m,j}^+ < 0$. See theorem 3.4(iv). Only for odd m and $j = 1$, the subsequent stabilization at $B_{m,1}^+ = 0$, \diamond , fails to occur at any finite control amplitude $\beta = 1/b < 0$.

Lemma 2.3. Consider $\tilde{\omega} > 0$, $\Omega = \tilde{\Omega} - \Omega_m$ with $\Omega_m = 2m + 1$, and $-1 < \Omega \leq 0$ for $m = 0$ but $-2 < \Omega \leq 0$ for $m \in \mathbb{N}$. Then the hashing relation $\tilde{\Omega} = \varepsilon \tilde{\omega}$, with $\varepsilon = \omega_k^{-1}$, is equivalent to

$$(2.21) \quad \Omega = \varepsilon(\omega + \frac{\pi}{2}(1 - (-1)^k - (-1)^m) - 2\pi j).$$

Here the representative $\omega = \tilde{\omega} \pmod{2\pi}$ is chosen such that

$$(2.22) \quad -\frac{\pi}{2} \leq \omega < \frac{3}{2}\pi,$$

$j \in \mathbb{N}$ is chosen such that

$$(2.23) \quad j = \begin{cases} 0 & \text{for } k, m \text{ both even,} \\ 1 & \text{otherwise,} \end{cases}$$

holds at $\Omega = 0$, and

$$(2.24) \quad \tilde{\omega} = \omega + 2\pi(km + [(k+1)/2] + [(m+1)/2] - j) \equiv \omega \pmod{2\pi}.$$

Proof. The hashing relations $\tilde{\Omega} = \varepsilon \tilde{\omega}$ and (2.21) are both affine linear in $\tilde{\omega}$, ω with slope ε . To show their equivalence, via $\tilde{\Omega} = \Omega + \Omega_m$ in (2.5) and definition (2.24) of ω , we only have to check (2.21) at $\varepsilon \tilde{\omega} = \tilde{\Omega} = \Omega_m$ and $\Omega = 0$. Indeed we obtain

$$(2.25) \quad \begin{aligned} \omega &:= \tilde{\omega} - 2\pi(km + [(k+1)/2] + [(m+1)/2] - j) = \\ &= \varepsilon^{-1} \cdot \Omega_m - \pi(2km + 2[(k+1)/2] + 2[(m+1)/2]) + 2\pi j = \\ &= (k + \frac{1}{2})\pi \cdot (2m + 1) - \pi(2km + k + m) + 2\pi j - \\ &\quad - \pi((2[(k+1)/2] - k) + (2[(m+1)/2] - m)) = \\ &= \frac{\pi}{2} + 2\pi j - \pi(\frac{1}{2}(1 - (-1)^k) + \frac{1}{2}(1 - (-1)^m)) = \\ &= 2\pi j - \frac{\pi}{2}(1 - (-1)^k - (-1)^m), \end{aligned}$$

as required by (2.21). The choice of j in (2.23) ensures the ranges (2.22) for $\Omega < 0$ near $\Omega = 0$. This proves the lemma. \bowtie

The Hopf points $B \in \mathbb{R}$, where purely imaginary eigenvalues $\mu = i\tilde{\omega} > 0$ arise, are therefore defined by the system of the 2-scale characteristic equation (2.20) and the hashing (2.21), in the precise sense of lemma 2.3. For the moment we “forget” hashing and address the complex 2-scale equation (2.20) first, in its own right. See also the bottom rows of figs. 2.1 and 2.2.

Lemma 2.4. The 2-scale characteristic equation $\chi_0(\delta, \omega, \Omega, B) = 0$ for purely imaginary eigenvalues, i.e. equation (1.25), (2.20), is equivalent to the system

$$(2.26) \quad \begin{aligned} 0 &= H(\delta, \Omega, \omega) := \tilde{\Omega} \sin(\frac{\pi}{2}\Omega) - (-1)^k \cos(\omega - \frac{\pi}{2}\Omega) = \\ &= (-1)^{m+1}(\tilde{\Omega} \cos(\frac{\pi}{2}\tilde{\Omega}) - (-1)^k \sin(\omega - \frac{\pi}{2}\tilde{\Omega})) \end{aligned}$$

$$(2.27) \quad B = (-1)^k \sin^2(\frac{\pi}{2}\Omega) / \cos \omega = (-1)^k \cos^2(\frac{\pi}{2}\tilde{\Omega}) / \cos \omega$$

with parameter $\delta = 1/(2m+1)$, $m \in \mathbb{N}_0$. As always, the case of even k results from odd k by addition of π to $\omega \pmod{2\pi}$. Here we have also used the previous notation

$$(2.28) \quad \tilde{\Omega} = \Omega + \Omega_m = \Omega + (2m+1) = \Omega + 1/\delta;$$

see (2.5). Eliminating $\omega \in (-\pi/2, 3\pi/2)$ we obtain the quadratic relation

$$(2.29) \quad 0 = Q(\delta, \Omega, B) := (\tilde{\Omega}^2 - 1)B^2 + \tilde{\Omega} \sin(\pi\tilde{\Omega})B + \cos^2(\frac{\pi}{2}\tilde{\Omega}).$$

The discriminant D of (2.29) is given by

$$(2.30) \quad D = \cos^2(\frac{\pi}{2}\tilde{\Omega}) \cdot (1 - (\tilde{\Omega} \cos(\frac{\pi}{2}\tilde{\Omega}))^2),$$

and the explicit solutions $B = B^\pm$ of (2.29) are

$$(2.31) \quad B^\pm = (\tilde{\Omega}^2 - 1)^{-1} (-\frac{1}{2}\tilde{\Omega} \sin(\pi\tilde{\Omega}) \pm \sqrt{D}).$$

For $m \in \mathbb{N}$ and $\Omega_m = 2m+1$, let $\underline{\tilde{\Omega}}_m \in (2m, \Omega_m)$ and $\tilde{\Omega}_m^{\max} \in (\Omega_m, 2m+2)$ denote the unique solutions $\tilde{\Omega}$ of $D = 0$, i.e. of

$$(2.32) \quad \tilde{\Omega} \cdot (-1)^m \cos(\frac{\pi}{2}\tilde{\Omega}) = 1,$$

in the respective intervals. In terms of $\Omega = \tilde{\Omega} - \Omega_m$ and $0 < \delta = \Omega_m^{-1}$ this defines unique solution branches (Ω, B^\pm) of (2.29) with

$$(2.33) \quad \begin{aligned} B^+ &< 0 < B^-, & \text{for } 0 =: \underline{\tilde{\Omega}}_0 < \tilde{\Omega} < \Omega_0 = 1, & m = 0; \\ B^\pm &< 0, & \text{for } \underline{\tilde{\Omega}}_m < \tilde{\Omega} < \Omega_m, & m \geq 1; \\ 0 &< B^\pm, & \text{for } \Omega_m < \tilde{\Omega} < \tilde{\Omega}_m^{\max}, & m \geq 1. \end{aligned}$$

Proof. For vanishing real part $\mu_R = 0$, the 2-scale characteristic equation (2.4) simplifies to

$$(2.34) \quad 0 = i\chi_0(\delta, \omega, \Omega, B) = i\tilde{\Omega} - (-1)^k e^{i\omega} - \frac{i}{B} \sin(\frac{\pi}{2}\Omega) e^{i\frac{\pi}{2}\Omega};$$

see (2.7), (2.20). To prove (2.26), we multiply by $\exp(-i\frac{\pi}{2}\Omega)$ and take real parts. To prove (2.27) we take real parts directly. To eliminate ω , as in (2.29), we solve $\chi_0 = 0$ in (2.34) for the only term $\exp(i\omega)$ which contains ω , and calculate the square of the absolute values of both sides. The remaining claims (2.30)–(2.33) concerning the quadratic relation (2.29) are plain high school calculus. This proves the lemma. \bowtie

In the following analysis we will skip the third case $m \geq 1$, $B^\pm > 0$, $\Omega_m < \tilde{\Omega} < \tilde{\Omega}_m^{\max}$ of (2.33) which is completely analogous to the second case $\underline{\tilde{\Omega}}_m < \tilde{\Omega} < \Omega_m$, $B^\pm < 0$. Indeed that third case will turn out to be irrelevant anyway, in section 3; see corollary 3.6.

Lemma 2.5. *The 2-scale relation (2.26) between slow and fast frequencies Ω and ω can be solved for $\Omega = \Omega(\delta, \omega)$, implicitly, and for the inverse function $\omega = \omega(\delta, \Omega)$, explicitly:*

$$(2.35) \quad \omega = \omega^\pm := \frac{\pi}{2}\Omega \pm \arccos(-\tilde{\Omega} \sin(\frac{\pi}{2}\Omega)) \pmod{2\pi},$$

for k odd. Even k require addition of $\pi \pmod{2\pi}$.

For $m = 0$, where $\delta = 1$ and $0 < \tilde{\Omega} = \Omega + 1 < 1$, both functions ω^\pm have strictly positive and bounded derivatives with respect to $\tilde{\Omega}$ or Ω , equivalently, in the interior domain. For odd k , their boundary values and ranges are, accordingly,

$$(2.36) \quad \begin{aligned} \omega^+ &\in [0, \frac{1}{2}\pi], \quad \text{with } \omega^+ = 0, \frac{1}{2}\pi \text{ at } \tilde{\Omega} = 0, 1; \\ \omega^- &\in [\pi, \frac{3}{2}\pi], \quad \text{with } \omega^- = \pi, \frac{3}{2}\pi \text{ at } \tilde{\Omega} = 0, 1. \end{aligned}$$

The ranges and boundary values are interchanged for even k . See the top row of fig. 2.1.

Let $m \geq 1$, where $0 < \delta = 1/(2m+1) \leq 1/3$, and consider $\underline{\Omega}_m \leq \tilde{\Omega} \leq 2m+1 = \Omega_m$; see (2.32). Then we observe ranges

$$(2.37) \quad \begin{aligned} \omega &\in [-\frac{\pi}{2}, \frac{\pi}{2}], \quad \text{for odd } k \geq 1, \\ \omega &\in [\frac{\pi}{2}, \frac{3}{2}\pi], \quad \text{for even } k \geq 2. \end{aligned}$$

Moreover, the implicit inverse function $\Omega = \Omega(\delta, \omega)$ is strictly piecewise monotone in ω with unique local and global minimum

$$(2.38) \quad -1 < \underline{\Omega}_m - \Omega_m =: \underline{\Omega}_m \leq \Omega \leq 0$$

and boundary values $\Omega = 0$ at $\omega \equiv \pm \frac{\pi}{2}$. The minimal value $\underline{\Omega}_m$ occurs at

$$(2.39) \quad \begin{aligned} \omega = \underline{\omega} &= \frac{\pi}{2}\underline{\Omega}_m && \text{for } k \text{ odd}, \\ \omega = \underline{\omega} &= \pi + \frac{\pi}{2}\underline{\Omega}_m && \text{for } k \text{ even}. \end{aligned}$$

The two explicit branches $\omega = \omega^\pm(\delta, \Omega)$ possess strictly nonzero, but only locally bounded, derivatives with respect to $\tilde{\Omega}$ or Ω , equivalently, in the domain $\underline{\Omega}_m < \Omega \leq 0$. They merge at $\Omega = \underline{\Omega}_m$, where the discriminant of the quadratic B -relation (2.29) vanishes. See the two upper rows of fig. 2.2.

Proof. As always, we may consider odd k , without loss. The explicit solutions $\omega = \omega^\pm$ of (2.35) follow directly from the 2-scale equation (2.26). Recall that nonnegative discriminants D in (2.30), (2.31) require $|\tilde{\Omega} \sin(\frac{\pi}{2}\Omega)| = |\tilde{\Omega} \cos(\frac{\pi}{2}\tilde{\Omega})| \leq 1$. Hence $-1 \leq \Omega \leq 0$ implies $-1 \leq \tilde{\Omega} \sin(\frac{\pi}{2}\Omega) \leq 0$. In particular $\arccos(-\tilde{\Omega} \sin(\frac{\pi}{2}\Omega)) \in [0, \frac{\pi}{2}]$, for all $m \in \mathbb{N}_0$. This proves claim (2.35) and the range claims (2.36), (2.37). Moreover the functions $\omega = \omega^\pm(\Omega)$ are differentiable with bounded derivatives, except for the vertical tangent at the discriminant loci $\Omega = \underline{\Omega}_m$, $m \geq 1$.

We study the monotonicity claims, for $m = 0$, and the convexity claims for the inverse function $\Omega = \Omega(\omega)$, for $m \geq 1$, next. Here we suppress δ , for a while. Recall $H(\Omega, \omega) = 0$, from (2.26). With the abbreviations

$$(2.40) \quad \begin{aligned} S &:= \sin(\tfrac{\pi}{2}\Omega) = -(-1)^m \cos(\tfrac{\pi}{2}\tilde{\Omega}), \\ C &:= \cos(\tfrac{\pi}{2}\Omega) = (-1)^m \sin(\tfrac{\pi}{2}\tilde{\Omega}), \\ s &:= \sin(\omega - \tfrac{\pi}{2}\Omega), \quad c := \cos(\omega - \tfrac{\pi}{2}\Omega), \end{aligned}$$

H and its partial derivatives for odd k , are

$$(2.41) \quad \begin{aligned} H &= \tilde{\Omega}S + c, \\ H_\Omega &= S + \tfrac{\pi}{2}\tilde{\Omega}C + \tfrac{\pi}{2}s, \\ H_\omega &= -s. \end{aligned}$$

Elementary arguments show that $H = 0$ is a regular value of H . Let $\dot{\Omega}$ denote the derivative of $\Omega(\omega)$. By implicit differentiation of $H(\Omega, \omega) = 0$ with respect to ω , we obtain

$$(2.42) \quad -H_\Omega \dot{\Omega} = H_\omega.$$

Suppose $\dot{\Omega} = 0$ at $\omega = \underline{\omega}$. Then

$$(2.43) \quad 0 = H_\omega = -s = -\sin(\omega - \tfrac{\pi}{2}\Omega)$$

at $\Omega = \Omega(\underline{\omega})$ implies $\omega = \underline{\omega} \equiv \tfrac{\pi}{2}\Omega \pmod{\pi}$. Insertion into $H(\Omega, \underline{\omega}) = 0$ implies

$$(2.44) \quad \pm 1 = -c = \tilde{\Omega}S = -(-1)^m \tilde{\Omega} \cos(\tfrac{\pi}{2}\tilde{\Omega}),$$

using (2.40). Since $S < 0$ we obtain $c = +1$. This implies $m \geq 1$ and

$$(2.45) \quad \tilde{\Omega} = \underline{\tilde{\Omega}}_m$$

as defined in (2.32). For $m = 0$, in fact, $0 \leq \tilde{\Omega} \leq 1$ prevents any solution of (2.44). This proves the strong monotonicity claims for $m = 0$, and completes the proof of lemma 2.5. \boxtimes

Lemma 2.6. *The functions $B^\pm = B^\pm(\delta, \Omega)$ for the control parameter B in (2.27), (2.29), (2.31) have the following properties.*

For $m = 0$, where $\delta = 1$ and $0 < \tilde{\Omega} = \Omega + 1 < 1$, we have

$$(2.46) \quad B^\pm(\delta, \Omega) = (-1)^k \frac{\sin^2(\tfrac{\pi}{2}\Omega)}{\cos \omega^\pm(\delta, \Omega)}.$$

Here ω^\pm have been defined in (2.35). Moreover B^+ increases strictly with respect to Ω , or $\tilde{\Omega}$,

$$(2.47) \quad \begin{aligned} B^+ &< 0 < B^- & \text{for } 0 < \tilde{\Omega} < 1; \\ B^+ &= -1, 0 & \text{for } \tilde{\Omega} = 0, 1; \\ B^- &= 1, \pi/2 & \text{for } \tilde{\Omega} = 0, 1. \end{aligned}$$

See the bottom row of fig. 2.1.

Let $m \geq 1$, where $0 < \delta < 1/(2m+1) \leq 1/3$ and $\underline{\tilde{\Omega}}_m \leq \tilde{\Omega} < 2m+1 = \Omega_m$; see (2.24). Then

$$(2.48) \quad \begin{aligned} B^- &< B^+ < 0; \\ B^\pm &= -\frac{1}{2}(\tilde{\Omega}_m^2 - 1)^{-1} \underline{\Omega}_m \sin(\pi \tilde{\Omega}_m), & \text{for } \tilde{\Omega} = \underline{\tilde{\Omega}}_m; \\ B^\pm &= 0, & \text{for } \tilde{\Omega} = \Omega_m. \end{aligned}$$

In terms of (2.39), the branches B^\pm are parametrized over ω , instead of Ω , as follows:

$$(2.49) \quad \begin{aligned} B^+ &= B(\delta, \omega), & \text{for } \omega > \underline{\omega} := \frac{\pi}{2} \underline{\Omega}_m; \\ B^- &= B(\delta, \omega), & \text{for } \omega < \underline{\omega} := \frac{\pi}{2} \underline{\Omega}_m. \end{aligned}$$

Moreover B^+ is strictly increasing with respect to ω , or Ω alias $\tilde{\Omega}$.

For B^- and $m \geq 1$ we encounter a zero derivative $\partial_\omega B^-$ at $\omega = \omega_*$, $\Omega = \Omega_*$ if, and only if,

$$(2.50) \quad 0 = d(\Omega, \omega) := \sin^2(\frac{\pi}{2} \Omega) \sin \omega + \frac{\pi}{2} \cos \omega \sin(\omega - \pi \Omega).$$

In particular, the minimum of B (and B^-) occurs at certain $\omega = \omega_*$, $\Omega = \Omega_*$ which satisfy

$$(2.51) \quad \pi \Omega_* < \omega_* < \frac{1}{2} \pi \Omega_* < 0.$$

Hence $\partial_\omega B^- < 0$ for $-\pi/2 < \omega < \pi \Omega_*$. Moreover $B > -1$.

Proof. Again we consider odd k , without loss. We suppress the parameter δ and differentiate (2.27) with respect to ω , implicitly, analogously to the proof of lemma 2.5:

$$(2.52) \quad \dot{B} = (-1)^k (\frac{\pi}{2} \sin(\pi \Omega) \cos \omega \cdot \dot{\Omega} + \sin^2(\frac{\pi}{2} \Omega) \sin \omega) / \cos^2 \omega.$$

We invoke lemma 2.5.

Consider $m = 0$, first. Then the sign of the right hand side of (2.46) is

$$(2.53) \quad -\text{sign } \cos \omega^\pm = \mp 1$$

by (2.36). These signs agree with our definition (2.31) of B^\pm , for $m = 0$, because $0 < \tilde{\Omega} < 1$ implies $B^+ < B^-$, there. More specifically, we have shown $B^+ < 0 < B^-$.

To settle monotonicity of B^+ , for all m , we keep considering odd k , without loss. We aim to show $\dot{B}^+ > 0$ in the interior domain of definition. We rewrite (2.52) as

$$(2.54) \quad \dot{B}^+ = -S(\pi C \cos \omega \cdot \dot{\Omega} + S \sin \omega) / \cos^2 \omega,$$

with $C > 0 > S$ for $-1 < \Omega < 0$; see (2.40) for this notation. Also recall $|\omega| < \pi/2$, $\cos \omega > 0$, $\dot{\Omega} > 0$ and $s = \sin(\omega - \frac{\pi}{2} \Omega) > 0$, for B^+ and odd k ; see the proof

of lemma 2.5. Therefore (2.54) implies $\dot{B}^+ > 0$, if $\sin \omega \leq 0$. It remains to show interior positivity of \dot{B}^+ for $\sin \omega > 0$, i.e. for $0 < \omega < \pi/2$.

Suppose $\dot{B} = 0$. We derive the relation (2.50) at such a zero, first. We differentiate $\chi_0 = 0$ in (2.7), (2.8) with respect to ω , implicitly, to obtain

$$(2.55) \quad 0 = \dot{\Omega} + e^{i\omega} + \frac{i}{2B} i\pi e^{i\pi\Omega} \dot{\Omega}.$$

We have used the assumption $\dot{B} = 0$ here. We multiply (2.55) by the complex conjugate coefficient of $\dot{\Omega}$ and take imaginary parts to eliminate the derivative $\dot{\Omega}$:

$$(2.56) \quad \begin{aligned} 0 &= \text{Im}(e^{i\omega}(1 - \frac{\pi}{2B}e^{-i\pi\Omega})) = \\ &= \sin \omega - \frac{\pi}{2B} \sin(\omega - \pi\Omega). \end{aligned}$$

Substitution of B from (2.27) and multiplication by the resulting denominator $\sin^2(\Omega\pi/2)$ proves claim (2.50).

We can now prove interior positivity $\dot{B}^+ > 0$ for the remaining case of $\sin \omega > 0$. Suppose $\dot{B}^+ = 0$, indirectly. We then use trigonometric addition and the abbreviations of (2.40) to rewrite (2.50) as

$$(2.57) \quad 0 = d(\Omega, \omega) = S^2 \sin \omega + \frac{\pi}{2} \cos \omega (-Sc + Cs).$$

Since $0 < \omega < \pi/2$, in the present case, the previous observations $-1 < \Omega < 0$ and $s > 0$ lead to strict positivity of all terms. This contradiction establishes $\dot{B}^+ > 0$ in all cases.

To prove claim (2.51), we first observe that $\omega < \frac{1}{2}\pi\Omega_m < \frac{1}{2}\pi\Omega < 0$ holds all along the ω^- -branch, because $-\pi/2 < \omega < \omega = \frac{1}{2}\pi\Omega_m$ defines the domain of B^- ; see lemma 2.5. To show $\omega_* > \pi\Omega_*$ at $\dot{B} = 0$, suppose $-\frac{\pi}{2} < \omega_* \leq \pi\Omega_* < 0$. We then claim $d(\Omega_*, \omega_*) < 0$. Indeed

$$(2.58) \quad \begin{aligned} d(\Omega_*, \omega_*) &= S_*^2 \sin \omega_* + \frac{\pi}{2} \cos \omega_* \sin(\omega_* - \pi\Omega_*) \leq \\ &\leq S_*^2 \sin \omega_* < 0. \end{aligned}$$

This contradiction proves (2.51).

It remains to prove $B > -1$, for $m \geq 1$. By continuity of B , and because $B^\pm = 0$ at $\tilde{\Omega} = \Omega_m = 2m + 1$, it is sufficient to show $B^- \neq -1$, indirectly. Suppose $B^- = -1$. Then $S^2 = \cos(\omega)$, by (2.27). Therefore (2.26) implies

$$(2.59) \quad \begin{aligned} 0 &= H/S = \tilde{\Omega} + \cos(\omega - \frac{\pi}{2}\Omega)/S = \\ &= \tilde{\Omega} + (C \cos \omega - S \sin \omega)/S = \\ &= \tilde{\Omega} + CS - \sin \omega \geq \tilde{\Omega} - 1 > 0, \end{aligned}$$

since $\tilde{\Omega} \geq \Omega_m - 1 = 2m \geq 2$. This proves $B > -1$, and completes the proof of the lemma. \boxtimes

3 Control-induced Hopf bifurcation

In absence of control, i.e. in the limit $b = 2\varepsilon B \rightarrow \pm\infty$, the original delay equation (1.4) possesses a trivial simple Hopf eigenvalue

$$(3.1) \quad \mu = i\tilde{\omega} = i\omega_k = i\varepsilon^{-1}$$

of the characteristic equation (2.1), at the original parameter

$$(3.2) \quad \lambda = \lambda_k = -(-1)^K/\varepsilon.$$

The (scaled) control parameter B induces further purely imaginary Hopf eigenvalues $\mu = \mu_R + i\tilde{\omega}$, $\mu_R = 0$, of the 2-scale characteristic equation (2.4). We fix and suppress $\delta = \Omega_m^{-1}$ in this section and rewrite (2.1)–(2.5) as

$$(3.3) \quad \begin{aligned} 0 = \psi(\mu, \varepsilon, B) &:= -\varepsilon B\mu - (-1)^k B e^{-\mu} + \frac{1}{2}(1 + e^{-\pi\varepsilon\mu}) = \\ &= -\varepsilon B\mu_R - iB\tilde{\Omega} - (-1)^k B e^{-\mu_R - i\tilde{\omega}} + \frac{1}{2}(1 + e^{-\pi\varepsilon\mu_R - i\pi\tilde{\Omega}}). \end{aligned}$$

As before we have abbreviated $\tilde{\Omega} = \Omega_m + \Omega = \delta^{-1} + \Omega$ here, and $\mu = \mu_R + i\tilde{\omega}$ with $\tilde{\omega} \equiv \omega \pmod{2\pi}$, $\varepsilon\tilde{\omega} = \tilde{\Omega}$. We also recall the hashing relation (1.23), i.e.

$$(3.4) \quad 0 = h(\tilde{\omega}, \Omega, \varepsilon) = -\tilde{\Omega} + \varepsilon\tilde{\omega} = -\Omega + \varepsilon(\omega + \frac{\pi}{2}(1 - (-1)^k - (-1)^m) - 2\pi j),$$

for $-\frac{\pi}{2} \leq \omega < \frac{3}{2}\pi$; see lemma 2.3. In other words, Hopf bifurcation is governed by the three real equations (3.3), (3.4) for vanishing $(\Psi, h) \in \mathbb{C} \times \mathbb{R}$, in the five not quite independent real variables $(\mu, \Omega, \varepsilon, B) \in \mathbb{C} \times \mathbb{R}^3$.

In trapping lemma 3.1 we observe absence of nontrivial eigenvalues $\mu = \mu_R + i\tilde{\omega}$ with imaginary parts $\tilde{\omega} \equiv \pm\pi/2 \pmod{2\pi}$. This traps imaginary parts in eigenvalue *strips*: an old and efficient idea already present in [BeCo63, Nu78]. It establishes the crucial sequences of Hopf bifurcations at scaled control parameters

$$(3.5) \quad B = B_{m,j}^{\pm},$$

where m, j label specific strips of the Hopf eigenvalues $\mu = i\tilde{\omega}$, with $\Omega_{m-1} < \tilde{\Omega} = \varepsilon\tilde{\omega} < \Omega_m = 2m + 1$.

We also observe how eigenvalues μ cannot appear from, or disappear towards, $\text{Re } \mu = +\infty$. Proposition 3.2 examines eigenvalues at vanishing control $b = 2B\varepsilon = \pm\infty$ to establish simplicity of eigenvalues, in each strip. With some estimates for Jacobian determinants involving Ψ and h , in proposition 3.3, we establish the transverse crossing directions of the simple Hopf eigenvalues μ , as B increases through $B_{m,j}^{\pm} < 0$; see the central crossing theorem 3.4 of this section. In fact we observe a gain of stability, i.e. decrease of the unstable dimensions $E = E(B)$ by 2, at $B = B_{m,j}^+ < 0$, and destabilization at $B_{m,j}^- < 0$. Corollary 3.5 concludes that Pyragas stabilization is impossible, for $B > 0$. Corollary 3.6 concludes that unstable eigenvalues in the complex (m, j) -strips are present if, and only if,

$$(3.6) \quad B_{m,j}^- < B < B_{m,j}^+.$$

Corollary 3.7 studies the case $m = 0$ of slow frequencies $0 < \tilde{\Omega} = \varepsilon\tilde{\omega} < 1$, as well as the simplest case $m = 1$. It concludes stability of the strip $m = 0$, $j = 1$ for $B_{0,1}^+ < B < 0$, but instability of the strip $m = 1$, $j = 1$ for $B_{1,1}^- < B < 0$. With the orderings of $B_{m,j}$ with respect to j , for each fixed $m \leq 1$, as collected in proposition 3.8 we arrive at the conclusion of this section, in corollary 3.9: the region $\mathcal{P} := \{B \mid B_{0,1}^+ < B < B_{1,1}^-\}$ is a nonempty Pyragas region, provided that

$$(3.7) \quad B_{m,j_m+1}^+ < B_{0,1}^+ < B_{1,1}^- < B_{m,j_m}^-$$

holds for $j_m := [(m+1)/2]$ and all $m \geq 1$. The ordering (3.7) will only be established in sections 4 and 5 below.

Lemma 3.1. *For any fixed $\varepsilon > 0$, consider strictly complex eigenvalues $\mu = \mu_R + i\tilde{\omega}$, i.e. solutions $\mu \in \mathbb{C} \setminus \mathbb{R}$ of the characteristic equation (3.3).*

(i) *Assume*

$$(3.8) \quad \mu_R \geq 0 > B.$$

Then the only eigenvalues $\mu = \mu_R + i\tilde{\omega}$ such that

$$(3.9) \quad 0 < \tilde{\omega} = \text{Im } \mu \equiv \frac{\pi}{2} \pmod{\pi}$$

are the trivial eigenvalues $\mu = i\omega_{\tilde{k}} = i(\tilde{k} + \frac{1}{2})\pi$ at $\varepsilon = \omega_{\tilde{k}}^{-1}$, where $\tilde{k} \in \mathbb{N}_0$ has the same parity as k .

(ii) *Assume*

$$(3.10) \quad \varepsilon = \omega_k^{-1}, \quad B \neq 0.$$

Then the only eigenvalue $\mu = \mu_R + i\tilde{\omega}$ such that

$$(3.11) \quad \tilde{\omega} = \omega_k = (k + \frac{1}{2})\pi$$

is the algebraically simple eigenvalue $\mu = i\omega_k$.

(iii) *Fix $\varepsilon = \omega_k^{-1}$, for some $k \in \mathbb{N}_0$, and fix any constant $K > 1$. Consider any sequence of (scaled) control parameters B_n and nontrivial eigenvalues $\mu_n = \mu_{R,n} + i\tilde{\omega}_n \neq i\omega_k$ such that*

$$(3.12) \quad \begin{aligned} 0 &\leq \mu_{R,n} \\ 1/K &\leq \tilde{\omega}_n \leq K, \quad \text{and} \\ B_n &\rightarrow 0. \end{aligned}$$

Then $|\mu_n|$ remains bounded. Moreover, for any convergent subsequence μ_n there exists a positive integer m such that

$$(3.13) \quad \begin{aligned} \varepsilon \lim \mu_n &= \lim \varepsilon i\tilde{\omega}_n = \lim i\tilde{\Omega}_n = i\Omega_m = i(2m+1), \quad \text{and} \\ \lim \tilde{\omega}_n \pmod{2\pi} &\equiv \begin{cases} \pi/2 & \text{for } k+m \text{ even,} \\ 3\pi/2 & \text{for } k+m \text{ odd.} \end{cases} \end{aligned}$$

Proof. To prove claim (i), suppose $\mu = \mu_R + i\tilde{\omega}$ with $\tilde{\omega} = \omega_{\tilde{k}} := (\tilde{k} + \frac{1}{2})\pi$, for some nonnegative integer \tilde{k} . We have to conclude $\mu_R = 0$ and $\varepsilon = \omega_{\tilde{k}}^{-1}$.

Abbreviating $\varepsilon\tilde{\omega} =: \tilde{\Omega}$, we decompose the characteristic equation (3.3) into real and imaginary parts at $\tilde{\omega} = \omega_{\tilde{k}}$ to obtain

$$(3.14) \quad -\varepsilon B\mu_R + \frac{1}{2}(1 + e^{-\pi\varepsilon\mu_R} \cos(\pi\tilde{\Omega})) = 0;$$

$$(3.15) \quad -B\tilde{\Omega} + (-1)^{k+\tilde{k}} B e^{-\mu_R} - \frac{1}{2} e^{-\pi\varepsilon\mu_R} \sin(\pi\tilde{\Omega}) = 0.$$

The real part (3.14) can be solved for $B\mu_R$ as

$$(3.16) \quad 0 \geq B\mu_R = \frac{1}{2}\varepsilon^{-1}(1 + e^{-\pi\varepsilon\mu_R} \cos(\pi\tilde{\Omega})) \geq 0.$$

Indeed, the right inequality follows because we have assumed $\mu_R \geq 0$ in (3.8), and the left inequality follows from our assumption $B < 0$. In particular we conclude

$$(3.17) \quad \mu_R = 0 \quad \text{and} \quad \cos(\pi\tilde{\Omega}) = -1.$$

Insertion of $\mu_R = 0$ and $\cos(\pi\tilde{\Omega}) = -1$, i.e. $\sin(\pi\tilde{\Omega}) = 0$, in the imaginary part (3.15) of (3.3) then implies

$$(3.18) \quad 0 > B\tilde{\Omega} = (-1)^{k+\tilde{k}} B e^{-\mu_R} = (-1)^{k+\tilde{k}} B.$$

This proves $\mu_R = 0$, $1 = \tilde{\Omega} = \varepsilon\omega_{\tilde{k}}$ and $k \equiv \tilde{k} \pmod{2\pi}$, as claimed.

To prove claim (ii), we first note

$$(3.19) \quad \tilde{\Omega} = \varepsilon\tilde{\omega} = \varepsilon\omega_k = 1, \quad \exp(-i\tilde{\omega}) = -(-1)^k i,$$

by assumptions (3.10), (3.11). For the imaginary part (3.15) of the characteristic equation (3.3) at $\mu = \mu_R + i\tilde{\omega}$ this implies

$$(3.20) \quad 0 = -B + B e^{-\mu_R},$$

i.e. $\mu_R = 0$.

To show algebraic simplicity of the resulting trivial eigenvalue $\mu = i\omega_k$ we differentiate the characteristic equation (3.3) with respect to μ there. A vanishing derivative requires

$$(3.21) \quad 0 = -\varepsilon B - iB + \frac{1}{2}\pi\varepsilon.$$

This contradiction proves algebraic simplicity of the trivial Hopf eigenvalue $\mu = \pm i\omega_k$ at $\varepsilon = \omega_k^{-1}$, for any B .

To prove claim (iii), we rewrite the characteristic equation (2.1) in the form

$$(3.22) \quad b_n(\varepsilon\mu_n + (-1)^k \exp(-\mu_n)) = 1 + \exp(-\pi\varepsilon\mu_n).$$

To show $|\mu_n|$ remains bounded, indirectly, we first suppose

$$(3.23) \quad |\mu_n| \rightarrow \infty,$$

for some subsequence. In (3.12) we have assumed bounded imaginary parts $\tilde{\omega}_n = \text{Im } \mu_n$. Therefore (3.8), (3.23) imply

$$(3.24) \quad \mu_{R,n} = \text{Re } \mu_n \rightarrow +\infty.$$

From (3.22) we then obtain, more precisely,

$$(3.25) \quad \lim \varepsilon b_n \mu_n = 1.$$

Taking imaginary parts of (3.22) and passing to a convergent subsequence of $\tilde{\omega}_n$, we also obtain

$$(3.26) \quad \begin{aligned} \lim \tilde{\omega}_n &= \lim \frac{\mu_n}{\varepsilon b_n \mu_n} \text{Im} \left(-(-1)^k b_n e^{-\mu_n} + e^{-\pi \varepsilon \mu_n} \right) = \\ &= \lim \mu_n \text{Im} \left(-(-1)^k b_n e^{-\mu_n} + e^{-\pi \varepsilon \mu_n} \right) = 0. \end{aligned}$$

This contradicts our lower bound (3.12) on $\tilde{\omega}_n$. Therefore the sequence $|\mu_n|$ is uniformly bounded.

Next we divide the original unscaled characteristic equation (2.1) for $\mu = \mu_n$ by $\varepsilon \mu_n - i \neq 0$, at $\varepsilon = \omega_k^{-1}$, to obtain

$$(3.27) \quad b_n \frac{\varepsilon \mu_n + (-1)^k \exp(-\mu_n)}{\varepsilon \mu_n - i} = \frac{1 + \exp(-\pi \varepsilon \mu_n)}{\varepsilon \mu_n - i}.$$

Both sides extend to entire functions of μ_n . Since (3.27) is entire, and $|\mu_n|$ remain bounded, $b_n \rightarrow 0$ then implies

$$(3.28) \quad \lim \frac{1 + \exp(-\pi \varepsilon \mu_n)}{\varepsilon \mu_n - i} = 0.$$

The denominator cancels the simple zero $\varepsilon \mu_n = i\Omega_0 = i$ of the numerator. The remaining zeros $\varepsilon \mu_n = i\Omega_m = i(2m+1)$ of the numerator prove claim (3.13), and the trapping lemma. \boxtimes

We now recall the location of eigenvalues μ of the characteristic equation (3.3) in the limit $B \rightarrow \pm\infty$ of vanishing control. This is well-known material; see e.g. [BeCo63, Hale77, Nu78]. We include a short proof for the convenience of the reader.

Proposition 3.2. *Consider eigenvalues $\mu \in \mathbb{C}$ at vanishing control $B = \pm\infty$, i.e. solutions of*

$$(3.29) \quad 0 = \varepsilon \mu + (-1)^k e^{-\mu}.$$

Then the following claims (i)–(iv) hold true.

(i) If $0 < \text{Im } \mu \equiv \pi/2 \pmod{\pi}$, then

$$(3.30) \quad \text{Re } \mu_R = 0, \quad \mu = i\omega_{\tilde{k}} = i(\tilde{k} + 1/2)\pi \quad \text{and} \quad \varepsilon = \omega_{\tilde{k}}^{-1},$$

where $\tilde{k} \in \mathbb{N}_0$ has the same parity as k .

(ii) At $\varepsilon = 1/\omega_k$ the eigenvalue $\mu = i\omega_k$ is algebraically simple. The local continuation $\mu = \mu(\varepsilon)$ satisfies

$$(3.31) \quad \frac{d}{d\varepsilon}\mu(0) = -\frac{1}{\varepsilon(1+\varepsilon^2)}(1+i\varepsilon).$$

(iii) For $1/\omega_k < \varepsilon < 1/\omega_{k-2}$ the nontrivial complex eigenvalues $\mu \in \mathbb{C} \setminus \mathbb{R}$ with $\operatorname{Re} \mu \geq 0$, $\operatorname{Im} \mu > 0$ are given by $[k/2]$ algebraic simple eigenvalues $\mu_{0,j}$, $j = 1, \dots, [k/2]$, one in each strip

$$(3.32) \quad \begin{aligned} 0 &< \operatorname{Re} \mu_{0,j}; \\ \omega_k - 2j\pi &< \operatorname{Im} \mu_{0,j} < \omega_k - 2j\pi + \frac{\pi}{2}. \end{aligned}$$

(iv) For even k , there do not exist real eigenvalues $\mu \geq 0$. If k is odd, the only real eigenvalue $\mu \geq 0$ is the algebraically simple eigenvalue defined by the unique positive solution of

$$(3.33) \quad \varepsilon\mu = e^{-\mu}.$$

Proof. Let $\mu = \mu_R + i\tilde{\omega}$. To prove claim (i), we first take real parts of (3.29) to see that $\cos \tilde{\omega} = 0$ implies $\mu_R = 0$. Taking imaginary parts,

$$(3.34) \quad \begin{aligned} 0 &= \varepsilon\omega_{\tilde{k}} - (-1)^k e^{-\mu_R} \sin \omega_{\tilde{k}} \\ &= \varepsilon\omega_{\tilde{k}} - (-1)^{k+\tilde{k}} \end{aligned}$$

shows the remaining claims of (i).

Claim (ii) follows by implicit differentiation of (3.29) with respect to ε :

$$(3.35) \quad 0 = \mu + (\varepsilon - (-1)^k e^{-\mu})\mu'$$

where μ' abbreviates the implicit derivative with respect to ε . Inserting $\varepsilon = \omega_k^{-1}$ and $\mu = i\omega_k$ proves claim (ii).

Claim (iii) follows by global continuation of the simple Hopf eigenvalues $\mu = \mu(\varepsilon)$ with respect to decreasing ε , alias increasing $|\lambda|$. We may proceed by induction on k . For large ε , i.e. for small λ alias small rescaled delay, already [Kur71] observed $\operatorname{Re} \mu \rightarrow -\infty$ for all complex eigenvalues. At $\varepsilon = \omega_{\tilde{k}}^{-1}$, with \tilde{k} of the same parity as k and $j := [\tilde{k}/2] + 1$, a simple Hopf eigenvalue $\mu = \mu_{0,j} := i\omega_{\tilde{k}}$ appears on the imaginary axis. By property (ii) it progresses, locally, for decreasing ε , into the strip (3.32). By property (i) that simple eigenvalue $\mu_{0,j}(\varepsilon)$ can never leave that trapping strip again, because $\operatorname{Re} \mu_{0,j} > 0$ remains bounded above for $\varepsilon > 0$ bounded below. By standard complex analysis, therefore, each $\mu_{0,j}(\varepsilon)$ remains simple and continues globally in its strip, for $0 < \varepsilon < \omega_{\tilde{k}}^{-1}$. The last k encountered for $\varepsilon > \omega_k^{-1}$ is $\tilde{k} = k - 2$. This proves claim (iii).

Claim (iv) on real eigenvalues μ has been addressed in lemma 2.1 already. This proves the proposition. \boxtimes

The following proposition collects the partial derivatives of the *characteristic function*

$$(3.36) \quad \psi(\mu, \varepsilon, B) := -\varepsilon B\mu - (-1)^k B e^{-\mu} + \frac{1}{2}(1 + e^{-\pi\varepsilon\mu})$$

introduced in (3.3).

Proposition 3.3. *The partial derivatives of $\psi = \psi(\mu, \varepsilon, B)$ satisfy*

$$(3.37) \quad \psi_\mu = -\varepsilon B + (-1)^k B e^{-\mu} - \frac{\pi}{2}\varepsilon e^{-\pi\varepsilon\mu};$$

$$(3.38) \quad \psi_\varepsilon = -\mu(B + \frac{\pi}{2}e^{-\pi\varepsilon\mu});$$

$$(3.39) \quad B\psi_B = -\varepsilon B\mu - (-1)^k B e^{-\mu} = \psi - \frac{1}{2}(1 + e^{-\pi\varepsilon\mu}).$$

At imaginary eigenvalues $\mu = i\tilde{\omega}$, where $\psi(\mu, \varepsilon; B) = 0$, and with the abbreviation $\tilde{\Omega} := \varepsilon\tilde{\omega}$, we also obtain the Jacobian determinant

$$(3.40) \quad -B \det \psi_{(\varepsilon, B)} = \tilde{\omega} \cdot (B + \frac{\pi}{2}) \cdot \cos^2(\frac{\pi}{2}\tilde{\Omega}).$$

Proof. The calculations of (3.37)–(3.39) are trivial. For $\psi = 0$ in (3.36) we also obtain

$$(3.41) \quad \psi_B = -\frac{1}{2B}(1 + e^{-\pi\varepsilon\mu}).$$

Since $\psi \in \mathbb{C} \cong \mathbb{R}^2$, the Jacobian $\psi_{(\varepsilon, B)}$ can be written abstractly as

$$(3.42) \quad \det \psi_{(\varepsilon, B)} = \det \begin{pmatrix} \operatorname{Re} \psi_\varepsilon & \operatorname{Re} \psi_B \\ \operatorname{Im} \psi_\varepsilon & \operatorname{Im} \psi_B \end{pmatrix} = \operatorname{Im} (\overline{\psi_\varepsilon} \cdot \psi_B).$$

Insertion of (3.38), (3.39), $\psi = 0$ at imaginary eigenvalues $\mu = i\tilde{\omega} = i\varepsilon^{-1}\tilde{\Omega}$ provides the Jacobian determinant

$$(3.43) \quad \begin{aligned} -B \det \psi_{(\varepsilon, B)} &= \operatorname{Im} (\overline{\psi_\varepsilon} \cdot (-B\psi_B)) = \\ &= \frac{1}{2}\tilde{\omega} \operatorname{Im} ((Bi + \frac{\pi}{2}ie^{i\pi\tilde{\Omega}})(1 + e^{-i\pi\tilde{\Omega}})) = \\ &= \frac{1}{2}\tilde{\omega} (B + \frac{\pi}{2})(1 + \cos(\pi\tilde{\Omega})). \end{aligned}$$

This proves (3.40) and the proposition. \bowtie

With these lengthy preparations we can now address transverse crossings at the relevant Hopf eigenvalues. Fix $\varepsilon = \omega_k^{-1}$ and consider nontrivial Hopf eigenvalues $\mu = i\tilde{\omega}$, $0 < \tilde{\omega} \neq \omega_k = (k + \frac{1}{2})\pi$, at control parameter $B \neq 0$. Equivalently,

$$(3.44) \quad \psi(\mu, \varepsilon, B) = 0$$

for ψ defined in (3.36); see (3.3).

In section 2 our view point was slightly different; see (2.20) and lemma 2.3. Hashing with the shifted slow frequency

$$(3.45) \quad \Omega = \tilde{\Omega} - \Omega_m = \varepsilon \tilde{\omega} - (2m + 1) = \varepsilon(\omega + \frac{\pi}{2}(1 - (-1)^k - (-1)^m) - 2\pi j),$$

$-\frac{\pi}{2} \leq \omega < \frac{3}{2}\pi$, $\omega \equiv \tilde{\omega} \pmod{2\pi}$, equivalently, we wrote the characteristic equation for the eigenvalue $\mu = i\tilde{\omega}$ as

$$(3.46) \quad 0 = \chi_0(\delta, \omega, \Omega, B) = \tilde{\Omega} + (-1)^k i e^{i\omega} - \frac{1}{B} \sin(\frac{\pi}{2}\Omega) e^{i\frac{\pi}{2}\Omega};$$

see (2.4)–(2.7). In lemma 2.5 we have described the solutions of (3.46) by functions

$$(3.47) \quad \Omega = \Omega(\omega),$$

for any fixed $\delta = \Omega_m^{-1}$ and nonnegative integers m . That description was completed with $B = B^\pm(\Omega) = B^\pm(\omega, \Omega(\omega))$ as

$$(3.48) \quad B = (-1)^k \sin^2(\frac{\pi}{2}\Omega) / \cos \omega = (-1)^k \cos^2(\frac{\pi}{2}\tilde{\Omega}) / \cos \omega;$$

see (2.27) and lemmata 2.4, 2.6.

We now combine these results, for $\varepsilon = \omega_k^{-1}$, with the hashing (3.45) to define the *Hopf frequencies* $\omega_{m,j}^\pm \in (-\frac{\pi}{2}, \frac{3}{2}\pi)$ as the intersections of (3.47) with (3.45), i.e.

$$(3.49) \quad \varepsilon(\omega_{m,j}^\pm + \frac{\pi}{2}(1 - (-1)^k - (-1)^m) - 2\pi j) = \Omega(\omega_{m,j}^\pm),$$

for $j = 1, \dots, j_m^{\max}$. Here and below we restrict attention to the case $\tilde{\Omega}_m \leq \tilde{\Omega} \leq \Omega_m$, i.e. $\underline{\Omega}_m \leq \Omega \leq 0$. Indeed, the opposite case of $m \geq 1$ and $B^\pm > 0$ of (2.33) will turn out irrelevant in corollary 3.6 below.

We have to comment on the precise meaning of (3.49), in view of lemma 2.5. Consider the case $m = 0$ first; see fig. 2.1. Since the derivatives of the two branches $\omega = \omega^\pm(\Omega)$ in (2.36) are bounded, their intersections with the near-vertical hashing lines $\tilde{\omega} = \tilde{\Omega}/\varepsilon$ of slope $1/\varepsilon$ are transverse, for $0 < \varepsilon \leq \varepsilon_0$ small enough. This provides two intersections $\omega = \omega_{0,j}^\pm$, one pair for each j , as indicated.

The cases $m \geq 1$ of fig. 2.2 are slightly more involved. The strictly decreasing lower branch $\omega = \omega^-(\Omega)$, $\underline{\Omega}_m < \Omega < 0$, is characterized by

$$(3.50) \quad -\pi/2 < \omega = \omega^-(\Omega) < \underline{\omega} = \frac{\pi}{2}\underline{\Omega}_m < 0.$$

This decreasing branch provides unique, transverse intersections $\omega = \omega_{m,j}^-$ with the increasing hashing lines. The strictly increasing upper branch $\omega = \omega^+(\Omega)$, $\underline{\Omega}_m < \Omega < 0$, on the other hand, may exhibit non-transverse, and even multiple, intersections $\omega \in \omega_{m,j}^+$ with the near-vertical hashing lines, for near-minimal $\Omega \gtrsim \underline{\Omega}_m$. This theoretical difficulty can be circumvented by certain tedious convexity arguments for $\Omega \gtrsim \underline{\Omega}_m$. Instead, we will simplify our presentation, mostly thinking of intersection *points* $\omega = \omega_{m,j}^+$, rather than intersection *sets* $\omega \in \omega_{m,j}^+$. Of course we will proceed

with the appropriate care to address the general set case whenever necessary. Finally, it will not be necessary to consider cases where the minimal intersection $\omega_{m,j}^-$ of the hashing line (m, j) belongs to the upper branch $\omega^+(\Omega)$; see lemma 5.4 below.

With these cautioning remarks in mind, we may proceed, mostly, with the additional requirement

$$(3.51) \quad \omega_{m,j}^- < \omega_{m,j}^+,$$

for $m \geq 1$. The only exception may arise by a tangency of the hashing, at maximal $j = \bar{j}_m$, $m \geq 1$, where $\omega_{m,j}^- = \min \omega_{m,j}^+$. We also note the exceptional boundary cases

$$(3.52) \quad \omega^\pm(-1) = 0, \quad \omega^-(0) \equiv \frac{\pi}{2} \pmod{\pi}, \quad \text{and } \omega^+(\Omega_m) \equiv \frac{\pi}{2} \pmod{\pi}, \quad m \geq 1,$$

for the functions $\omega^\pm(\Omega)$ of lemma 2.5 which we discuss separately below. Let us keep in mind how $\omega_{m,j}^\pm$ come with their shifted and slow variants

$$(3.53) \quad \tilde{\omega}_{m,j}^\pm, \quad \tilde{\Omega}_{m,j}^\pm, \quad \Omega_{m,j}^\pm$$

as an entourage; see (3.45). These also define the control parameters

$$(3.54) \quad B = B_{m,j}^\pm = (-1)^k \cos^2\left(\frac{\pi}{2} \tilde{\Omega}_{m,j}^\pm\right) / \cos \omega_{m,j}^\pm$$

where the nontrivial, control-induced Hopf bifurcations with eigenvalues $\mu = \pm i \tilde{\omega}_{m,j}^\pm$ actually occur.

Theorem 3.4. *With the above notation, the following holds, at $\varepsilon = \omega_k^{-1}$.*

(i) *The values $B_{0,j}^\pm$ of the control parameter enumerate all nontrivial Hopf bifurcations with eigenvalues $\mu = \pm i \tilde{\omega}$ of frequencies $0 < \tilde{\omega} < \omega_k = (k + \frac{1}{2})\pi$.*

(ii) *The values $B_{m,j}^\pm$ with $m \geq 1$ enumerate all nontrivial Hopf bifurcations with eigenvalue frequencies $\tilde{\omega} > \omega_k$ and strictly negative control parameter $B < 0$.*

(iii) *All enumerated Hopf eigenvalues are algebraically simple.*

(iv) *The local continuations $\mu = \mu_{m,j}^-(B)$ of all enumerated Hopf eigenvalues $i\omega_{m,j}^- = \mu_{m,j}^-(B_{m,j}^-)$ cross the imaginary axis transversely with*

$$(3.55) \quad \frac{d}{dB} \operatorname{Re} \mu_{m,j}^-(B) > 0$$

at $B = B_{m,j}^-$. At $B = \max B_{m,j}^+$, generated by the frequencies $\omega_{m,j}^+$, that unstable eigenvalue recovers stability, at the latest.

Proof. The proof of claims (i) and (ii) follows from our detailed analysis of the characteristic equation $\chi_0 = 0$ in section 2; see in particular lemma 2.4.

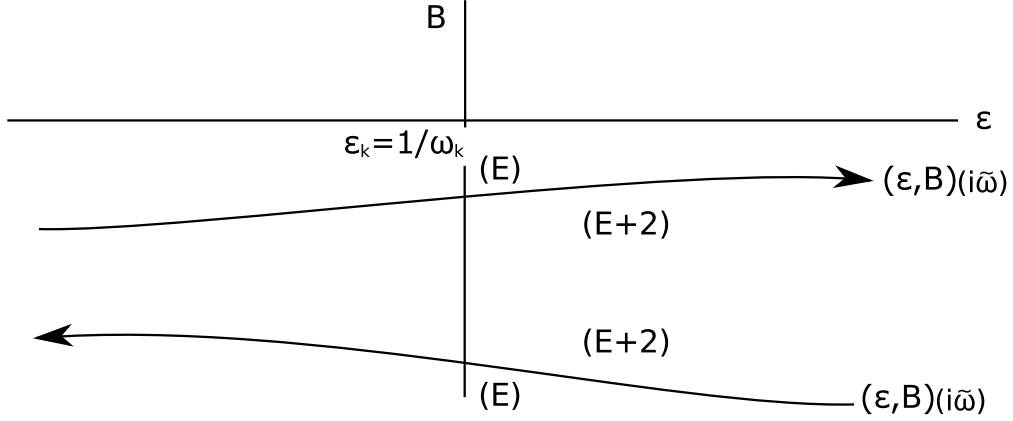


Figure 3.1: Hopf curves $\tilde{\omega} \mapsto (\varepsilon(i\tilde{\omega}), B(i\tilde{\omega}))$, oriented along increasing $\tilde{\omega}$. Note the resulting unstable dimensions E , in parantheses, to the left, and $E + 2$ to the right, of the Hopf curves.

To prove simplicity of Hopf eigenvalues, (iii), we partially substitute the explicit expression (2.27) for B into ψ_μ of (3.37), and take real parts:

$$\begin{aligned}
 \text{Re } \psi_\mu &= -\varepsilon B + (-1)^k B \cos \tilde{\omega} - \frac{\pi}{2} \varepsilon \cos(2\frac{\pi}{2}\tilde{\Omega}) = \\
 (3.56) \quad &= -\varepsilon B + \cos^2(\frac{\pi}{2}\tilde{\Omega}) - \frac{\pi}{2} \varepsilon (2 \cos^2(\frac{\pi}{2}\tilde{\Omega}) - 1) = \\
 &= \varepsilon(\frac{\pi}{2} - B) + (1 - \pi\varepsilon) \cos^2(\frac{\pi}{2}\tilde{\Omega}) > 0
 \end{aligned}$$

for $\pi\varepsilon = \pi\omega_k^{-1} = 1/(k + 1/2)$, $k \geq 1$, and all enumerated B . Indeed, by lemma 2.6, the only exception to $B \leq \pi/2$ arises for $B = \pi/2$ at the excluded trivial eigenvalue with frequency $\tilde{\omega} = \tilde{\Omega}/\varepsilon = 1/\varepsilon = \omega_k$. This proves simplicity claim (iii).

For $m \geq 1$, our proof of the remaining crossing and (de)stabilization claims (iv) will be based on the following three ingredients. We will first invoke the implicit function theorem to show that the local continuation map

$$(3.57) \quad (\varepsilon, B) \mapsto \mu = \mu(\varepsilon, B)$$

is an orientation preserving diffeomorphism, near $\varepsilon = \omega_k^{-1}$ and the enumerated Hopf eigenvalues $\mu = i\omega_{m,j}^\pm$ at $B = B_{m,j}^\pm$. In a second step we will then show

$$(3.58) \quad \varepsilon_\omega(i\omega_{m,j}^-) < 0$$

for the partial derivatives, with respect to ω , of the local inverse function $(\varepsilon, B) = (\varepsilon(\mu), B(\mu))$ to (3.57), at $\mu = i\omega_{m,j}^-$. The third ingredient describes the necessary adaptations at $\omega_{m,j}^+$.

We first show how claims (3.57) and (3.58) imply the crossing direction

$$(3.59) \quad \text{Re } \mu_B > 0,$$

for the partial derivative of $\mu(\varepsilon, B)$ with respect to B at $\mu = i\omega_{m,j}^-$. Indeed consider the oriented Hopf curve $\tilde{\omega} \rightarrow (\varepsilon(i\tilde{\omega}), B(i\tilde{\omega}))$ in the (ε, B) plane. See fig. 3.1. By the

orientation preserving transformation (3.57), the region $\operatorname{Re} \mu < 0$ lies to the left of the Hopf curve. By (3.58), the tangent to the Hopf curve at $\omega = \omega_{m,j}^-$ points strictly to the left of the vertical B -axis at the fixed value $\varepsilon = \varepsilon_k$. Therefore, the B -axis crosses the Hopf curve transversely, at $\omega = \omega_{m,j}^-$, and into the unstable region $\operatorname{Re} \mu > 0$, for increasing B . Thus the diffeomorphism (3.57) implies (3.59).

The cases $B = B_{m,j}^+$ can be treated analogously, with a little extra care. In the case of a single transverse crossing of the hashing line (m, j) with the upper branch $\omega = \omega^+(\Omega)$, at $\omega = \omega_{m,j}^+$, we now have $\varepsilon_\omega(i\omega_{m,j}^+) > 0$. Therefore, the tangent to the Hopf curve at $\omega = \omega_{m,j}^+$ now points strictly to the right of the vertical B -axis at the fixed value $\varepsilon = \varepsilon_k$. The previous arguments then show $\operatorname{Re} \mu_B < 0$, i.e. stabilization towards increasing B . In case of multiple crossings, possibly involving tangents, we can prove stabilization from the last crossing (or tangency) onwards, as claimed in (iv), via generic approximation by an odd number of transverse crossings of the hashing line with the upper branch $\omega = \omega^+(\Omega)$. Put simply, destabilization occurs whenever the increasing hashing lines in the top rows of fig. 2.2 enter the interior region of the 2-scale relation $\Omega = \Omega(\delta, \omega)$, and stabilization ensues as soon as the hashing lines leave towards the exterior region; see lemma 2.5.

To prove claim (iv) for $m \geq 1$ it therefore remains to verify claims (3.57) and (3.58). We will address the analogous, but simpler, case $m = 0$ at the end of the proof.

To verify the orientation claim (3.57) we invoke the implicit function theorem for $\psi(\mu, \varepsilon, B) = 0$; see (3.3), (3.36). Indeed the Jacobian determinants, which determine the local orientations, satisfy

$$(3.60) \quad \det \psi_\mu \cdot \det \mu_{(\varepsilon, B)} = \det(-\psi_{(\varepsilon, B)}) = \det(\psi_{(\varepsilon, B)}).$$

Our enumeration of cases $B = B_{m,j}^\pm$ for $m \geq 1$ above has skipped any positive B^\pm of lemma 2.4, (2.33). By lemma 2.6 we know $-1 < B^- \leq 0$. Therefore proposition 3.3, (3.40) asserts strict positivity of $\det(\psi_{(\varepsilon, B)})$ in (3.60). The enumerated Hopf eigenvalues $\mu = i\omega_{m,j}^\pm$ are simple zeros of the complex analytic characteristic function $\psi \in \mathbb{C}$, by claim (iii). Therefore $\det \psi_\mu$ on the left is also strictly positive, by the Cauchy-Riemann equations. This proves strict positivity of $\det \mu_{(\varepsilon, B)}$ and establishes the orientation claim (3.57).

To determine the signs of the tangent partial derivatives ε_ω , as claimed in (3.58), we recall the definition

$$(3.61) \quad \varepsilon = \tilde{\Omega}/\tilde{\omega} = \tilde{\Omega}(\tilde{\omega})/\tilde{\omega},$$

where $\tilde{\Omega}(\tilde{\omega}) = \Omega_m + \Omega(\omega)$ follows from the ε -independent characteristic equation $\chi_0(\delta, \omega, \Omega, B) = 0$ at $\omega \equiv \tilde{\omega} \pmod{2\pi}$, for fixed $\delta = \Omega_m^{-1}$. See (3.46), (3.47) and lemmata 2.4, 2.5. Straightforward differentiation of (3.61) with respect to $\tilde{\omega} > 0$ or ω yields

$$(3.62) \quad \begin{aligned} \varepsilon_\omega &= (\dot{\Omega} - \tilde{\Omega}/\tilde{\omega})/\tilde{\omega} = \\ &= (\dot{\Omega} - \varepsilon)/\tilde{\omega}, \end{aligned}$$

in the notation of lemma 2.5, where $\dot{\Omega} = d\Omega/d\omega = d\tilde{\Omega}/d\tilde{\omega}$. The definition of $\omega_{m,j}^-$ as the unique intersection of the hashing line (m, j) with the lower branch $\omega = \omega^-(\Omega)$ in (3.45), and (3.49), (3.50) show that (3.62) implies the sign of ε_ω claimed in (3.58). See the two top rows of fig. 2.2. The case of a single transverse crossings at $\omega = \omega_{m,j}^+$ leads to $\varepsilon_\omega(i\omega_{m,j}^+) > 0$, analogously. The required adaptations for multiple and/or non-transverse crossings have been described above.

It remains to address the case $m = 0$, $0 < \tilde{\Omega} < 1$. Consider $\omega_{0,j}^+$, $B_{0,j}^+ < 0$ first; see lemmata 2.4–2.6. Here each crossing $\omega = \omega_{m,j}^\pm$ is transverse and unique. Transformation (3.57) remains orientation preserving, by (3.40) and (3.60), verbatim as for $m \geq 1$. Furthermore (3.62) implies $\varepsilon_\omega > 0$, for small enough $0 < \varepsilon < \varepsilon_0$, by an upper bound on the positive derivatives

$$(3.63) \quad 0 < 1/\dot{\Omega} = \frac{d}{d\Omega}\omega^\pm(\Omega) < 1/\varepsilon_0$$

in lemma 2.5. This shows claim (iv), (3.55) at $B = B_{0,j}^+ < 0$, for $m = 0$. To show claim (iv), (3.55) at $B = B_{0,j}^- > 0$, for $m = 0$, we first note that (3.40), (3.60) now imply orientation reversal in (3.57), because

$$(3.64) \quad \det \psi_{(\varepsilon, B)} < 0.$$

The argument (3.63), however, remains intact at $\omega^-(\Omega)$. This shows how the sign reversal claimed in (iv), (3.55) remains valid for $m = 0$, proving the lemma. \bowtie

Figs. 2.1 and 2.2 already summarized our results, so far, separately for $m = 0$ and for $m \geq 1$, $B < 0$. Consider the case $m = 0$ first, i.e. slow Hopf frequencies $0 < \tilde{\Omega} < \Omega_0 = 1$, alias $-1 < \Omega = \tilde{\Omega} - \Omega < 0$. The branch $\omega = \omega^+(\Omega)$ of Hopf frequencies $\omega \equiv \tilde{\omega} \pmod{2\pi}$ provides

$$(3.65) \quad k' = [k/2]$$

Hopf bifurcations at control parameters $B = B_{0,j}^+$, $j = 1, \dots, k'$. Hashing and strong monotonicity of $B = B^+(\Omega)$, lemma 2.6, imply

$$(3.66) \quad \begin{aligned} -1 &< \Omega_{0,k'}^+ < \dots < \Omega_{0,2}^+ < \Omega_{0,1}^+ < 1; \\ -1 &< B_{0,k'}^+ < \dots < B_{0,2}^+ < B_{0,1}^+ < 0. \end{aligned}$$

By lemma 3.1, unstable eigenvalues $\mu = \mu_R + i\tilde{\omega}$ cannot cross any of the lines $\tilde{\omega} \equiv \pi/2 \pmod{\pi}$, for $B < 0$. By proposition 3.2, each of the $k' = [k/2]$ resulting strips

$$(3.67) \quad \operatorname{Re} \mu > 0, \quad 0 < \omega_k - 2j\pi < \tilde{\omega} < \omega_k - 2j\pi + \pi,$$

$j = 1, \dots, k'$, contains exactly one simple eigenvalue $\mu_{0,j}$ inherited from $B = -\infty$. By theorem 3.4 and analytic continuation, this simple eigenvalue persists as B increases, until it disappears into $\operatorname{Re} \mu < 0$ by simple transverse Hopf bifurcation at

$$(3.68) \quad B = B_{0,j}^+, \quad \tilde{\omega} = \omega_{0,j}^+.$$

Indeed $\tilde{\omega} = \omega_{0,j}^+$ belongs to the same strip (3.67), for each $j = 1, \dots, k'$. For even $k = 2k'$, this eliminates all unstable eigenvalues generated at $B = -\infty$, once

$$(3.69) \quad B_{0,1}^+ < B < 0.$$

For odd $k = 2k' + 1$, the same statement remains true, because $-1 < B < 0$ renders the additional real eigenvalue stable; see lemma 2.1 and corollary 2.2. Note $-1 < B_{0,1}^+$ here, by lemma 2.6; see also fig. 2.1. These remarks prove the following corollary.

Corollary 3.5. *Let $\varepsilon = 1/\omega_k$ and assume $B < 0$. Then $\mu_R < 0$ for any eigenvalue $\mu = \mu_R + i\tilde{\omega}$ with $0 \leq \tilde{\omega} < \omega_k$, if and only if (3.69) holds.*

We study $B > 0$ next. In corollary 2.2 we have already observed instability, by parity due to the presence of a real eigenvalue $\mu > 0$, in case k was odd. Let us therefore consider even $k = 2k'$. At $\varepsilon = 1/\omega_k$ and $B = +\infty$ we encounter the same k' unstable simple complex eigenvalues $\mu_{0,j}$, one in each of the k' strips (3.67), as before. This time, however, only $k' - 1$ simple transverse Hopf bifurcation points $B = B_{0,j}^- > 0$ offer their assistance for stabilization by decreasing $B > 0$. Indeed $B_{0,j}^-$ cancels the instability of $\mu_{0,j+1}$, for $j = 1, \dots, k' - 1$, but $\mu_{0,k'}$ remains unstable for all $B > 0$. This proves the following corollary.

Corollary 3.6. *Let $\varepsilon = 1/\omega_k$ and assume $B > 0$. Then there exists an unstable eigenvalue μ , i.e. $\text{Re } \mu > 0$. For odd k , the unstable eigenvalue can be taken to be real. For even $k \geq 2$, the unstable eigenvalue $\mu = \mu_R + i\tilde{\omega}$ can be taken to be strictly complex with*

$$(3.70) \quad 0 < \omega_k - 2\pi < \tilde{\omega} < \omega_k - \pi.$$

In particular, there does not exist any region of Pyragas stabilization (near Hopf bifurcation) for control parameters $B > 0$.

Henceforth we restrict attention to the remaining case $B < 0$. We fix $\varepsilon = 1/\omega_k$. All unstable real eigenvalues, or complex eigenvalues $\mu = \mu_R + i\tilde{\omega}$ with $0 < \tilde{\omega} < \omega_k$ come from $B = -\infty$ and have been taken care of in corollary 3.5. By the trapping lemma 3.1 for imaginary parts, all remaining changes of stability must arise from the simple transverse Hopf bifurcations at

$$(3.71) \quad B = B_{m,j}^\pm, \quad m \geq 1,$$

as enumerated in theorem 3.4. Note how the imaginary parts $\tilde{\omega} > 0$ of any unstable eigenvalues $\mu = \mu_R + i\tilde{\omega}$ induced by these Hopf bifurcations are confined to the disjoint strips

$$(3.72) \quad \tilde{\omega} = \omega + 2\pi(km + [(k+1)/2] + [(m+1)/2] - j)$$

where $\pi/2 < \omega < 3\pi/2$ for even k , and $-\pi/2 < \omega < \pi/2$ for odd k . This follows from hashing (2.24), (3.49) at Hopf bifurcation frequencies $\tilde{\omega} = \tilde{\omega}_{m,j}^\pm$, and persists with instability of μ , by trapping lemma 3.1 of imaginary parts. In particular, the strips are disjoint, for different (m, j) , and $B_{m,j}^\pm$ generate frequencies $\tilde{\omega}_{m,j}^\pm$ which remain in the same strip. See also fig. 2.2. This proves the following corollary.

Corollary 3.7. *Let $0 < \varepsilon = 1/\omega_k \leq \varepsilon_0$ be sufficiently small, and assume $B < 0$. Then there exists an unstable eigenvalue μ , i.e. $\operatorname{Re} \mu > 0$, if at least one of the following conditions holds:*

$$(3.73) \quad \begin{aligned} & B < B_{0,1}^+ < 0, \quad \text{or} \\ & B_{m,j}^- < B < \min B_{m,j}^+ \leq 0, \end{aligned}$$

for some $m \geq 1$ and some j enumerated in theorem 3.4. Here we define $B_{m,1}^+ := 0$ for odd m .

We have implicitly excepted hashing tangencies $\Omega_{m,j}^- = \min \tilde{\Omega}_{m,j}^+$ in equation (2.48). Indeed this case corresponds to a nontransverse Hopf point, at (scaled) frequency $\tilde{\Omega}_{m,j}^- = \min \tilde{\Omega}_{m,j}^+$, from the stable side. This does not contribute to the strict unstable dimension $E(B)$.

Hence we may assume $\tilde{\Omega}_{m,j}^- < \tilde{\Omega}_{m,j}^+$. Then hashing (3.49) implies $B_{m,j}^- < B_{m,j}^+$. Indeed this follows from strong monotonicity of $B^+(\Omega)$ in case $\Omega_{m,j}^\pm = \Omega(\omega_{m,j}^\pm)$ with $\omega_{m,j}^\pm \geq \underline{\omega}$; see lemma 2.6. If $\omega_{m,j}^- < \underline{\omega} < \omega_{m,j}^+$, then we reach the same conclusion, again by strong monotonicity of $B^+(\tilde{\Omega})$ and lemma 2.4:

$$(3.74) \quad B_{m,j}^- = B^-(\Omega_{m,j}^-) < B^+(\Omega_{m,j}^-) < B^+(\Omega_{m,j}^+) = B_{m,j}^+.$$

More systematically, these arguments are collected in the following proposition.

Proposition 3.8. *Let $\varepsilon = 1/\omega_k \leq \varepsilon_0$ be sufficiently small. For any $m \geq 1$ consider the enumeration of Hopf bifurcation parameters $B_{m,j}^\pm$ of theorem 3.4. Then*

$$(3.75) \quad B_{m,j}^- < B_{m,j}^+ < 0,$$

except at a possible hashing tangency $\Omega_{m,j}^- = \min \Omega_{m,j}^+$. Moreover the series $B_{m,j}^+$ decreases strictly monotonically in $j = 1, \dots, j_m^{\max}$, for each fixed $m \geq 1$.

Proof. Claim (3.75) has been proved in (3.74). Strict monotonicity of $B_{m,j}^+ = B^+(\Omega_{m,j}^+)$ in j follows from strict monotonicity of $\tilde{\Omega}_{m,j}^+ = \tilde{\omega}_{m,j}^+/\varepsilon$ in the j -strips (3.72) and from strict monotonicity of $\Omega \mapsto B^+(\Omega)$ in lemma 2.6. This proves the proposition. \boxtimes

We summarize the results of this section in a final corollary. Define

$$(3.76) \quad j_m := [(m+1)/2],$$

for integer $m \geq 1$. In the following sections we will show, for small enough $0 < \varepsilon = 1/\omega_k \leq \varepsilon_0$, that $B_{0,1}^+$ is unique, and

$$(3.77) \quad \max B_{m,j_m+1}^+ < B_{0,1}^+ < 0 \quad \text{for} \quad j_m + 1 \leq j_m^{\max},$$

i.e. as long as Ω_{m,j_m+1}^+ exists. See (3.49) for the delimiter $j = 1, \dots, j_m^{\max}$ of the enumeration $B_{m,j}^\pm$. On the other hand, we will also show

$$(3.78) \quad B_{0,1}^+ < B_{1,1}^- < 0, \quad \text{and}$$

$$(3.79) \quad B_{1,1}^- \leq B_{m,j}^- < 0, \quad \text{for } j = 1, \dots, \min\{j_m, j_m^{\max}\}.$$

This identifies the Pyragas region \mathcal{P} as follows.

Corollary 3.9. *Let $0 < \varepsilon = 1/\omega_k \leq \varepsilon_0$ be chosen small enough and assume the orderings (3.77)–(3.79), for all $m \geq 1$. Then the nonempty Pyragas region*

$$(3.80) \quad \mathcal{P} = \{B < 0 \mid B_{0,1}^+ < B < B_{1,1}^-\}$$

is the only region of control parameters $B = \frac{1}{2}b/\varepsilon$ in the delay equation (1.17), such that Pyragas stabilization succeeds for the Hopf bifurcation at $\lambda = \lambda_k = (-1)^{k+1}\varepsilon^{-1}$.

Proof. By corollary 3.6, instability prevails for all $B > 0$. By corollary 3.7, instability holds for $B < B_{0,1}^+$, and for $B_{1,1}^- < B < 0$. It therefore remains to show that

$$(3.81) \quad (B_{m,j}^-, \max B_{m,j}^+) \cap (B_{0,1}^+, B_{1,1}^-) = \emptyset,$$

for all $m \geq 1$ and $j = 1, \dots, j_m^{\max}$.

Strong monotonicity of $B_{m,j}^+$ with respect to j , as in proposition 3.8, and assumption (3.77) imply

$$(3.82) \quad \max B_{m,j}^+ \leq \max B_{m,j_m+1}^+ < B_{0,1}^+$$

for all $m \geq 1$ and $j > j_m$. This establishes claim (3.81) for $j_m < j \leq j_m^{\max}$, provided that $j_m < j_m^{\max}$.

It remains to show claim (3.81) for $1 \leq j \leq \min\{j_m, j_m^{\max}\}$. In this case we invoke assumption (3.79) to conclude an empty intersection (3.81), again. Since the Pyragas region (3.80) is nonempty, by assumption (3.78), this proves the corollary. \bowtie

4 Locally uniform expansions in $\varepsilon = 1/\omega_k$

To locate and understand the Pyragas region

$$(4.1) \quad \mathcal{P} = \{B \mid B_{0,1}^+ < B < B_{1,1}^-\},$$

in the limit $\varepsilon = 1/\omega_k \rightarrow 0$ of Hopf bifurcations with large unstable dimensions k , it remains to establish the precise locations of the control induced Hopf bifurcations $B_{m,j}^\pm$ relative to the gap (4.1). See assumptions (3.77)–(3.79) of corollary 3.9. In the present section we accomplish this task, by expansions with respect to small ε , for arbitrary bounded $m = 1, \dots, m_0$ alias $\delta \geq \delta_0 := 1/\Omega_{m_0} = 1/(2m_0 + 1)$.

To be precise, we first fix any $m_0 \in \mathbb{N}$, alias $\delta_0 > 0$. In section 5, we will choose δ_0 sufficiently small. In the present section we will then consider $0 < \varepsilon \leq \varepsilon_0 = \varepsilon_0(\delta_0)$ small enough for certain ε -expansions of $B_{m,j}^\pm$ to hold, uniformly for all $m \leq m_0$ and $j \leq j_m + 1$, $j_m = [(m+1)/2]$. Note how the derivatives of $\omega^\pm(\Omega)$ remain bounded in the relevant region; see (4.2). Hence $\omega_{m,j}^\pm$ and $B_{m,j}^\pm$ are defined uniquely by transverse intersections of the 2-scale characteristic equation (2.26) with the hashing lines $\tilde{\omega} = \tilde{\Omega}/\varepsilon$ of (4.5), (4.6), in the present section.

In particular, the ε -expansions of $B_{0,1}^+$ and $B_{1,1}^-$ will establish the expansions (1.19) of $\underline{b}_k = 2\varepsilon B_{0,1}^+$ and $\bar{b}_k = 2\varepsilon B_{1,1}^-$; see (1.28). The limit $\delta \rightarrow 0$ of large $m \rightarrow \infty$ uses a different approach will be deferred to the next section.

Our strategy has been outlined in (1.23)–(1.28). We first solve the ε -independent 2-scale characteristic equation $H(\Omega, \omega) = 0$ of (2.26) for $\omega = \omega(\Omega)$ explicitly:

$$(4.2) \quad \omega = \omega^\pm(\Omega) = \frac{\pi}{2}\Omega \pm \arccos(-\tilde{\Omega} \sin(\frac{\pi}{2}\Omega));$$

see lemma 2.5. Here and below we only consider odd k , without loss of generality, up to an addition of π . Recall $|\omega| \leq \pi/2$, for odd k . We also recall $\tilde{\Omega} = 1/\delta + \Omega$ and

$$(4.3) \quad 0 \leq -\tilde{\Omega} \sin(\frac{\pi}{2}\Omega) \leq 1,$$

by the discriminant condition (2.32). Equivalently

$$(4.4) \quad 0 \geq \Omega \geq \underline{\Omega}_m.$$

Note bounded derivatives of $\omega(\Omega)$, locally uniformly for $0 \geq \Omega > \underline{\Omega}_m$. We suppress explicit dependence on δ , m , in the present section.

Next we insert (4.2) into the hashing relation (2.21) of lemma 2.3:

$$(4.5) \quad \Omega = \varepsilon(\omega^\pm(\Omega) - a\pi)$$

with the abbreviation

$$(4.6) \quad a = a_{m,j} = 2j - 1 + \frac{1}{2}(-1)^m.$$

Here we have used that k is odd; the relevant modifications for even k cancel in (4.5) and below. By the implicit function theorem we can solve (4.5) for

$$(4.7) \quad \Omega = \Omega(\varepsilon, a) = \Omega_{m,j}^\pm(\varepsilon),$$

uniquely, for small enough $0 < \varepsilon \leq \varepsilon_0 = \varepsilon_0(\delta_0)$. Inserting the result into ω^\pm of (4.2) and B of (2.27) we obtain expansions

$$(4.8) \quad \begin{aligned} \omega &= \omega_{m,j}^\pm(\varepsilon) := \omega^\pm(\Omega_{m,j}^\pm(\varepsilon)), \\ B &= B_{m,j}^\pm(\varepsilon) := -\sin^2(\frac{\pi}{2}\Omega_{m,j}^\pm(\varepsilon))/\cos \omega_{m,j}^\pm(\varepsilon). \end{aligned}$$

We collect these straightforward expansions in the following proposition.

Proposition 4.1. *For any fixed $\delta_0 = 1/\Omega_{m_0} > 0$ consider $0 < \varepsilon \leq \varepsilon_0 = \varepsilon_0(\delta_0)$ small enough. Then the expansions for $\Omega_{m,j}^\pm$, $\omega_{m,j}^\pm$, and $B_{m,j}^\pm$ with respect to ε are*

$$(4.9) \quad \begin{aligned} \Omega_{m,j}^-(\varepsilon) &= -(4j + (-1)^m - 1)\frac{\pi}{2}\varepsilon + 2m(4j + (-1)^m - 1)\left(\frac{\pi}{2}\varepsilon\right)^2 + \dots; \\ \Omega_{m,j}^+(\varepsilon) &= -(4j + (-1)^m - 3)\frac{\pi}{2}\varepsilon - 2(m+1)(4j + (-1)^m - 3)\left(\frac{\pi}{2}\varepsilon\right)^2 + \dots; \end{aligned}$$

$$(4.10) \quad \begin{aligned} \omega_{m,j}^-(\varepsilon) &= -\frac{\pi}{2} + 2m(4j + (-1)^m - 1)\left(\frac{\pi}{2}\varepsilon\right)^2 + \dots; \\ \omega_{m,j}^+(\varepsilon) &= \frac{\pi}{2} - 2(m+1)(4j + (-1)^m - 3)\left(\frac{\pi}{2}\varepsilon\right)^2 + \dots; \end{aligned}$$

$$(4.11) \quad \begin{aligned} B_{m,j}^-(\varepsilon) &= -\frac{1}{2m}(4j + (-1)^m - 1)\left(\frac{\pi}{2}\varepsilon\right)^2 + \\ &\quad + \left(\frac{1}{2m}\right)^2(4j + (-1)^m - 1)(4m^2 - 4j - (-1)^m + 1)\left(\frac{\pi}{2}\varepsilon\right)^3 + \dots; \\ B_{m,j}^+(\varepsilon) &= -\frac{1}{2(m+1)}(4j + (-1)^m - 3)\left(\frac{\pi}{2}\varepsilon\right)^2 - \left(\frac{1}{2(m+1)}\right)^2(4j + (-1)^m - 3) \cdot \\ &\quad \cdot (4m^2 + 8m + 4j + (-1)^m + 1)\left(\frac{\pi}{2}\varepsilon\right)^3 + \dots. \end{aligned}$$

The expansions for B^\pm , Ω^\pm hold for even and odd k , alike. The expansions for ω^\pm are given for odd k . For even k , we have to add π ; see lemma 2.5.

Proof. We omit the obvious calculation. \(\boxtimes\)

Corollary 4.2. *In the setting of proposition 4.1 we obtain the following expansions and inequalities, for $0 < \varepsilon \rightarrow 0$:*

$$(4.12) \quad B_{1,1}^- = -\left(\frac{\pi}{2}\right)^2\varepsilon + \left(\frac{\pi}{2}\right)^3\varepsilon^2 + \dots$$

$$(4.13) \quad B_{0,1}^+ = -\left(\frac{\pi}{2}\right)^2\varepsilon - 3\left(\frac{\pi}{2}\right)^3\varepsilon^2 + \dots$$

$$(4.14) \quad 0 > B_{m,1}^- > B_{m,2}^- > B_{m,3}^- > \dots$$

For $m \geq 1$ and $j_m := [(m+1)/2]$ we obtain the expansion

$$(4.15) \quad B_{m,j_m}^- = -\left(\frac{\pi}{2}\right)^2\varepsilon + (2m-1)\left(\frac{\pi}{2}\right)^3\varepsilon^2 + \dots$$

$$(4.16) \quad B_{m,j_m+1}^+ = -\left(\frac{\pi}{2}\right)^2\varepsilon - (2m+3)\left(\frac{\pi}{2}\right)^3\varepsilon^2 + \dots$$

Proof. The proof follows from proposition 4.1, by explicit evaluation. \(\boxtimes\)

Corollary 4.3. *The assumptions (3.77)–(3.79) of corollary 3.9 are satisfied for all $1 \leq m \leq m_0$ and sufficiently small $0 < \varepsilon \leq \varepsilon_0$. In particular, expansions (4.12), (4.13) determine the ε -expansions (1.19) of the boundaries \underline{b}_k , \bar{b}_k of the Pyragas region, in our main theorem 1.2.*

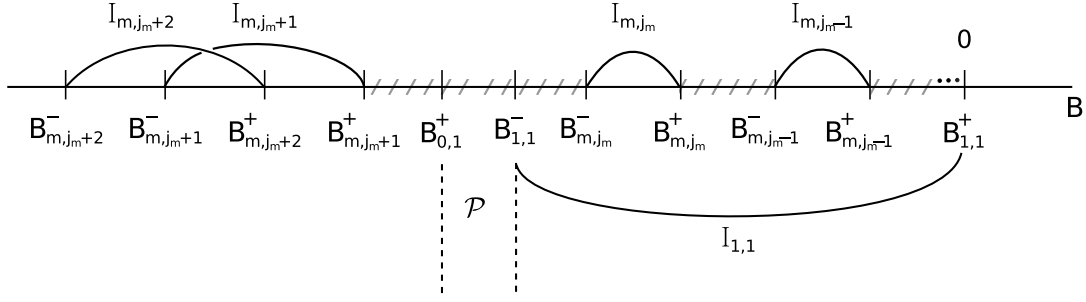


Figure 4.1: Stability windows (hashed) between intervals $I_{m,j} = (B_{m,j}^-, B_{m,j}^+)$ of Hopf-induced unstable eigenvalues with imaginary parts in the disjoint intervals designed by m, j . Note how the first, leftmost, stability window between I_{m,j_m+1} and I_{m,j_m} contains the only Pyragas region $\mathcal{P} = (B_{0,1}^+, B_{1,1}^-)$ of stable supercritical Hopf bifurcation, for any m such that I_{m,j_m+1} still exists.

Proof. Claim (3.77) follows by comparison of the expansion (4.16) for B_{m,j_m+1}^+ with expansion (4.13) for $B_{0,1}^+$, for $1 \leq m \leq m_0$. Likewise (4.12), (4.15), and (4.14), in this order, imply

$$(4.17) \quad B_{1,1}^- \leq B_{m,j_m}^- < B_{m,j_m-1}^- < \dots < B_{m,1}^-.$$

This proves claim (3.79). The remaining claim $B_{0,1}^+ < B_{1,1}^-$ of (3.78) is immediate by comparison of the respective expansions (4.12) and (4.13). This proves the corollary. \square

For $m \geq 1$, there is an amusing characterization of the critical index $j = j_m = \lfloor (m+1)/2 \rfloor$ as a *Pyragas switch index*, in our expansions. In fact our ε -expansions (4.11) easily imply

$$(4.18) \quad \begin{aligned} B_{m,j+1}^+ &< B_{m,j}^- & \text{for } j = 1, \dots, j_m, \\ B_{m,j+1}^+ &> B_{m,j}^- & \text{for } j > j_m. \end{aligned}$$

The interpretation is easy. Consider the open intervals $B \in I_{m,j} := (B_{m,j}^-, B_{m,j}^+)$ at Hopf-induced unstable eigenvalues $\mu = \mu_R + i\tilde{\omega}$, $\mu_R > 0$, with frequency $\tilde{\omega}$ trapped in the disjoint intervals designated by m, j ; see lemma 3.1, and (4.5), (4.6) with $|\omega| \leq \pi/2$. Then (4.18) states that successive instability intervals $I_{m,j}$ and $I_{m,j+1}$ leave a stability window in between, for $j \leq j_m$, but overlap for $j > j_m$. See fig. 4.1. In view of (4.17), therefore, the stability window

$$(4.19) \quad B_{m,j_m+1}^+ < B < B_{m,j_m}^-$$

is the very first stability window encountered, between the instability intervals $I_{m,j}$, $m \geq 1$, as j decreases from j_m^{\max} to 1, i.e. as $B < 0$ increases towards zero from absent control at $B = -\infty$.

The instability inherited from $B = -\infty$, on the other hand, is only compensated for once $B_{0,1}^+ < B < 0$, by the stabilizing series of Hopf bifurcations in the $m = 0$

series at $B = B_{0,j}^+$. The instability interval $I_{1,1} = (B_{1,1}^-, B_{1,1}^+)$ which starts from $B_{1,1}^- > B_{0,1}^+$, however, extends all the way to $B_{1,1}^+ = 0$. Therefore any stability windows between the intervals $I_{m,j}$ of instability, for $m \geq 1$ and j from $j_m + 1$ down to 1, remain ineffective. The only exception is the first such gap (4.19) which, somewhat miraculously, contains the Pyragas region \mathcal{P} of (3.80) by (3.77), (3.79) as established above.

We are somewhat amazed how all these gaps align, simultaneously for all resonance orders m , at the same first order location

$$(4.20) \quad B = -(\frac{\pi}{2})^2 \varepsilon + \dots,$$

to contribute to Pyragas stabilization from $B = B_{0,1}^+$ to $B = B_{1,1}^-$ by a second order effect. We will see next how such gaps also arise in the remaining limit $\delta \rightarrow 0$ of large $m \rightarrow +\infty$.

5 Asymptotic expansions for large $\Omega_m = 1/\delta$

In the previous section we have shown how the series of destabilizing Hopf intervals $B \in I_{m,j} := (B_{m,j}^-, B_{m,j}^+)$ skip the Pyragas candidate

$$(5.1) \quad \mathcal{P} = (B_{0,1}^+, B_{1,1}^-),$$

for bounded values $m \leq m_0$, accordingly bounded $j \leq j_m^{\max}$, and small enough $\varepsilon = 1/\omega_k \leq \varepsilon_0(\delta_0)$. In other words, we have established assumptions (3.77)–(3.79) of corollary 3.9, for bounded $m \leq m_0$ and $0 < \varepsilon \leq \varepsilon_0(\delta_0)$. In the present section we will complete this analysis, for large $m > m_0$.

In section 4, we had fixed m, j , to study ε -expansions of $B_{m,j}^\pm$. We also noticed the central role of

$$(5.2) \quad j = j_m := [(m+1)/2],$$

where the Pyragas switch (4.19) actually did occur, between B_{m,j_m+1}^+ and B_{m,j_m}^- . This suggests a somewhat delicate parametrization of the relevant expansions by ε and $\delta := 1/\Omega_m = 1/(2m+1)$, both tending to zero in a region $\delta \geq \delta(\varepsilon)$. Instead, we choose a parametrization of the problem by a rectangular region of (δ, ω) . The ε -independent relations $\Omega^\pm = \Omega(\delta, \omega)$, $B^\pm = B(\delta, \omega)$ will provide expansions with respect to small δ . At $j = j_m$ for B_{m,j_m}^- , and at $j = j_m + 1$ for B_{m,j_m+1}^+ , we will also obtain expansions for

$$(5.3) \quad \varepsilon = \varepsilon(\delta, \omega),$$

from the hashing relation (4.5). In other words, we determine ε such that B_{m,j_m}^- and B_{m,j_m+1}^+ arise at the frequency parameter ω , for some small δ . The ε -expansions for the Pyragas boundary $B_{0,1}^+(\varepsilon)$, $B_{1,1}^-(\varepsilon)$, in section 4, did not depend on δ . They will allow us to compare the resulting locations, now, uniformly for small $0 < \delta \leq \delta_0$. This will prove our main theorem, via corollary 3.9.

We address the general case in lemma 5.1. The limits $\omega \rightarrow \pm\pi/2$, for $B_{m,j}^\pm$, will be considered in lemma 5.2. These results address the cases where B_{m,j_m}^- , B_{m,j_m+1}^+ actually exist, and $\omega_{m,j_m}^- < \pi\Omega_{m,j_m}^-$. The remaining cases where $j_m \geq j_m^{\max}$ are prepared by expansions for $\min B$, in proposition 5.3, and are resolved in lemma 5.4.

As in section 4, we may restrict our attention to odd k , $|\omega| \leq \pi/2$. See also (4.3), (4.4). We mostly replace m by $\delta = 1/\Omega_m = 1/(2m+1)$ and think of $0 < \delta \leq \delta_0$ and $0 < \varepsilon \leq \varepsilon_0(\delta_0)$ as small continuous, rather than discrete, real variables in all expansions. For example

$$(5.4) \quad 2j_m = 2[(m+1)/2] = \frac{1}{2}(\delta^{-1} - (-1)^m),$$

$$(5.5) \quad a_{m,j_m} := 2j_m - 1 + \frac{1}{2}(-1)^m = \frac{1}{2}\delta^{-1} - 1,$$

for the Pyragas switch index $j = j_m$ of (4.19), (5.2) and the associated shift $a = a_{m,j_m}$ in hashing (4.5), (4.6).

Our δ -expansions are based on section 2. From lemmata 2.5, 2.6 we recall how the 2-scale characteristic equation in the form

$$(5.6) \quad (\delta^{-1} + \Omega) \sin(\frac{\pi}{2}\Omega) + \cos(\omega - \frac{\pi}{2}\Omega) = 0,$$

$$(5.7) \quad B = -\sin^2(\frac{\pi}{2}\Omega) / \cos \omega,$$

of (2.6), (2.27) gives rise to unique functions $\Omega = \Omega(\delta, \omega)$, $B = B(\delta, \omega)$, successively. Insertion into hashing

$$(5.8) \quad \varepsilon = \Omega / (\omega - \pi a_{m,j_m})$$

with (5.4), (5.5) then provides $\varepsilon = \varepsilon^-(\delta, \omega)$, such that we encounter

$$(5.9) \quad B = B_{m,j_m}^-(\delta, \omega) \quad \text{at} \quad \varepsilon = \varepsilon^-(\delta, \omega),$$

for $-\pi/2 < \omega \leq \underline{\Omega}_m \pi/2$. Similarly, the hashing

$$(5.10) \quad \varepsilon = \Omega / (\omega - \pi a_{m,j_m+1}),$$

with $a_{m,j_m+1} = a_{m,j_m} + 2$ in (5.5), provides $\varepsilon = \varepsilon^+(\delta, \omega)$ such that we encounter

$$(5.11) \quad B = B_{m,j_m+1}^+(\delta, \omega) \quad \text{at} \quad \varepsilon = \varepsilon^+(\delta, \omega)$$

for $\underline{\Omega}_m \pi/2 \leq \omega < \pi/2$. The established ε -expansions of the Pyragas boundaries $B_{0,1}^+(\varepsilon)$, $B_{1,1}^-(\varepsilon)$ of corollary 4.2, (4.12) and (4.13), finally, at $\varepsilon = \varepsilon^\pm(\delta, \omega)$, respectively, allow us to compare these δ -expansions as required in assumptions (3.77) and (3.79) of corollary 3.9.

Note how any possible nonuniqueness within the sets $B_{m,j}^+$ is remedied by our parametrization: we neither claim nor require injectivity of $\omega \mapsto \varepsilon_{m,j}^+(\delta, \omega)$, for fixed δ .

Lemma 5.1. *For odd k , and uniformly in $|\omega| \leq \pi/2$, we obtain the following expansions with respect to small δ :*

$$(5.12) \quad \Omega(\delta, \omega) = -\frac{c}{\pi/2}(\delta - s\delta^2 + \dots)$$

$$(5.13) \quad B(\delta, \omega) = -c(\delta^2 - 2s\delta^3 + \dots)$$

$$(5.14) \quad \varepsilon^\pm(\delta, \omega) = (\frac{\pi}{2})^{-2}c(\delta^2 + (\frac{\omega}{\pi/2} \mp 2 - s)\delta^3 + \dots)$$

$$(5.15) \quad B_{0,1}^+(\delta, \omega) = -c(\delta^2 + (\frac{\omega}{\pi/2} - 2 - s)\delta^3 + \dots)$$

$$(5.16) \quad B_{1,1}^-(\delta, \omega) = -c(\delta^2 + (\frac{\omega}{\pi/2} + 2 - s)\delta^3 + \dots)$$

Here we used the abbreviations $c = \cos \omega$, $s = \sin \omega$. Omitted terms are of the first omitted integer order in δ .

Proof. To see why we obtain a uniform expansion of Ω , we rewrite (5.6) in the equivalent form

$$(5.17) \quad \sin(\frac{\pi}{2}\Omega) = -c \cos(\frac{\pi}{2}\Omega)\delta/(1 + \delta(\Omega + s)).$$

For $0 \leq \delta \leq \delta_0$, the implicit function theorem provides $\Omega = \Omega(\delta, \omega)$, uniformly in ω . Note the important uniform prefactor $c = \cos \omega$ in

$$(5.18) \quad \Omega = (\Omega/\sin(\frac{\pi}{2}\Omega)) \cdot \sin(\frac{\pi}{2}\Omega) = -c\delta \cdot (\dots),$$

because $\Omega/\sin(\Omega\pi/2)$ is regular nonzero. To obtain the specific expansion (5.12) for Ω we solve (5.6) for δ , expand for Ω at $\Omega = 0$, and invert the resulting series for

$$(5.19) \quad \begin{aligned} \delta &= -\sin(\frac{\pi}{2}\Omega)/(\cos(\omega - \frac{\pi}{2}\Omega) + \Omega \sin(\frac{\pi}{2}\Omega)) \\ &= -\frac{\pi/2}{c}\Omega + \dots \end{aligned}$$

To obtain expansion (5.13) for $B = -\sin^2(\Omega\pi/2)/c$ we insert (5.12) into (5.7) and observe cancellation of the denominator c . Indeed we pick up a factor c^2 from (5.12) in the numerator. This proves (5.13). Of course (5.13) applies to all $B_{m,j}^\pm = B(\delta, \omega)$, identically, at the appropriate values ω .

The expansions (5.14) for ε^\pm follow from the hashings (5.8)–(5.11), if we replace a_{m,j_m} and $a_{m,j_m+1} = a_{m,j_m+2}$ by their appropriate δ -dependent values $1/(2\delta) \pm 1$ from (5.5). The prefactor c remains inherited from Ω .

To prove claims (5.15), (5.16) it only remains to plug (5.14) into the ε -expansions (4.12) and (4.13) for $B_{1,1}^-$ and $B_{0,1}^+$. Note how the new term of order δ^3 , which roughly speaking corresponds to $\varepsilon^{3/2}$, arises from the leading term $-(\pi/2)^2\varepsilon^\pm + \dots$ alone. This proves the lemma. \boxtimes

Lemma 5.2. *Let $0 < \delta \leq \delta_0$ be small enough and consider odd k . Let $\Omega, B, \varepsilon^\pm, B_{0,1}^+, B_{1,1}^-$ be expanded as in lemma 5.1.*

Then, somewhat paradoxically at first sight, we obtain the inequalities

$$(5.20) \quad B_{1,1}^-(\delta, \omega) < B(\delta, \omega) < B_{0,1}^+(\delta, \omega),$$

for all $0 < \delta \leq \delta_0$, $|\omega| < \pi/2$.

For $j_m + 1 \leq j_m^{\max}$ and at $\varepsilon = \varepsilon^+(\delta, \omega)$ we conclude, in particular,

$$(5.21) \quad B_{m, j_m+1}^+ < B_{0,1}^+(\delta, \omega),$$

i.e. assumption (3.77) of corollary 3.9 holds. Likewise, for $j_m \leq j_m^{\max}$ and at $\varepsilon = \varepsilon^-(\delta, \omega)$ we conclude

$$(5.22) \quad B_{1,1}^-(\delta, \omega) < B_{m, j_m}^-.$$

Under the additional assumption

$$(5.23) \quad -\pi/2 < \omega_* \leq \pi\Omega(\delta, \omega_*),$$

we can also assert $-\pi/2 < \omega \leq \pi\Omega(\delta, \omega)$, for all $-\pi/2 \leq \omega \leq \omega_*$. Moreover

$$(5.24) \quad \omega \mapsto B(\delta, \omega) < 0$$

is then strictly decreasing, for fixed δ and all $-\pi/2 \leq \omega \leq \omega_*$.

For example suppose (5.23) holds at $\Omega(\delta, \omega_*) = \Omega_{m, j_*}^-$, $\omega_* = \omega^-(\Omega_{m, j_*}^-)$, for some $1 \leq j_* \leq j_m^{\max}$, $m \geq 1$. Then

$$(5.25) \quad B_{m, j_*}^- < \dots < B_{m, 1}^- \leq 0$$

holds at $\varepsilon = \varepsilon(\delta, \omega_*)$, for all $1 \leq j \leq j_*$. For the above ranges of ε, δ , this establishes the Pyragas region \mathcal{P} , via assumptions (3.77), (3.79) of corollary 3.9.

Proof. To prove claim (5.20), we first divide (5.20) by $c = \cos \omega > 0$ and compare with expansions (5.13), (5.15), (5.16) of lemma 5.1. For $|\omega| < \pi/2 - \eta_0$ bounded away from $\pi/2$, the claim (5.20) becomes equivalent to the obvious inequalities

$$(5.26) \quad \begin{aligned} \frac{\omega}{\pi/2} + 2 - s &> -2s > \frac{\omega}{\pi/2} - 2 - s, \quad \text{i.e.} \\ \frac{\omega}{\pi/2} + 2 &> -s > \frac{\omega}{\pi/2}. \end{aligned}$$

Equality holds for $\omega = -\pi/2$, on the left, and for $\omega = +\pi/2$, on the right. Therefore $\eta_0 = 0$ does not seem an option for proving (5.20), uniformly for small δ , at first. However, we obtain uniform expansions for the partial derivatives $\partial_\omega B_{0,1}^+$, $\partial_\omega B_{1,1}^-$, $\partial_\omega B$ as well, by differentiation of the coefficients of (5.15), (5.16), (5.13). At $\omega = -\pi/2$ we obtain

$$(5.27) \quad \partial_\omega((B - B_{1,1}^-)/c) = \partial_\omega(s + \frac{\omega}{\pi/2} + 2)\delta^3 + \dots = \frac{1}{\pi/2}\delta^3 + \dots > 0,$$

and at $\omega = +\pi/2$, similarly,

$$(5.28) \quad \partial_\omega((B_{0,1}^+ - B)/c) = \partial_\omega(-\frac{\omega}{\pi/2} + 2 - s)\delta^3 + \dots = -\frac{1}{\pi/2}\delta^3 + \dots < 0.$$

This establishes positivity of the differences for all $|\omega| < \pi/2$, uniformly for all $0 < \delta \leq \delta_0$, and settles claim (5.20).

To prove claim (5.21) we invoke $B(\delta, \omega) < B_{0,1}^+(\delta, \omega)$ from (5.20). In fact

$$(5.29) \quad B_{m,j_m}^- = B(\delta, \omega), \quad B_{m,j_m+1}^+ = B(\delta, \omega),$$

in our parametrization, for any $m \geq 1$. Note how (5.29) refers to possibly different $\varepsilon = \varepsilon^\pm(\delta, \omega)$ given by (5.8), (5.9) and (5.10), (5.11), respectively. Indeed ε has been eliminated in the 2-scale characteristic equations (5.6), (5.7), and only enters after the (m, j) -dependent hashings (5.8), (5.10). Thus (5.21) holds by definition of $\varepsilon^+(\delta, \omega)$. The arguments for (5.22) via $\varepsilon^-(\delta, \omega)$ are completely analogous.

To complete the proof we only have to establish the strict monotonicity of $\omega \mapsto B(\delta, \omega)$ and of $B_{m,j}^-$, $j = 1, \dots, j_*$ as claimed in (5.24), (5.25). We invoke lemmata 2.5 and 2.6. By lemma 2.5 we have strictly decreasing dependence $\Omega \mapsto \omega^-(\delta, \Omega)$, for fixed $\delta > 0$. By lemma 2.6, assumption (5.23) implies strict decrease of $\omega \mapsto B(\delta, \omega)$, as long as $\omega \leq \pi\Omega(\delta, \omega)$. By monotonicity of Ω , we remain in this region, for all smaller $\omega \geq -\pi/2$, once we are ever inside. This proves claim (5.24).

Specifically, suppose assumption (5.23) holds for $\omega_* = \omega^-(\delta, \Omega_{m,j_*}^-)$, and hence for all $-\pi/2 \leq \omega \leq \omega_* = \omega^-(\delta, \Omega_{m,j_*}^-)$. Then conclusion (5.24) holds for all $-\pi/2 \leq \omega \leq \omega_* = \omega^-(\delta, \Omega_{m,j_*}^-)$. Hashing (5.8) implies strict monotonicity of slow frequencies,

$$(5.30) \quad \Omega_{m,j_*}^- < \dots < \Omega_{m,1}^- \leq 0.$$

In particular (5.30) successively implies

$$(5.31) \quad \begin{aligned} \omega_* &= \omega^-(\Omega_{m,j_*}^-) > \dots > \omega^-(\Omega_{m,1}^-) \geq -\pi/2, \\ B(\delta, \omega_*) &= B_{m,j_*}^- < \dots < B_{m,1}^- \leq 0, \end{aligned}$$

at $\varepsilon = \varepsilon(\delta, \omega_*)$. This proves claim (5.25), and the lemma. \boxtimes

We now address the remaining segment of the piecewise strictly monotone curve $\omega \mapsto \Omega(\delta, \omega)$, where

$$(5.32) \quad \pi\Omega(\delta, \omega) \leq \omega \leq \frac{\pi}{2}\Omega(\delta, \omega) < 0.$$

By lemma 2.6, this segment contains

$$(5.33) \quad B_{\min}(\delta) = \min_{|\omega| \leq \pi/2} B(\delta, \omega).$$

Proposition 5.3. *Let k be odd. Uniformly, for ω satisfying (5.32), we have the expansions*

$$(5.34) \quad \Omega(\delta, \omega) = -\frac{1}{\pi/2}\delta + \mathcal{O}(\delta^3);$$

$$(5.35) \quad B(\delta, \omega) = -\delta^2 + \mathcal{O}(\delta^4).$$

In particular this implies

$$(5.36) \quad B_{\min}(\delta) = -\delta^2 + \mathcal{O}(\delta^4).$$

Proof. We invoke the expansions (5.12) and (5.13) of lemma 5.1. Indeed (5.12) and (5.32) imply

$$(5.37) \quad -2c\delta + \dots = \pi\Omega(\delta, \omega) \leq \omega \leq \frac{\pi}{2}\Omega(\delta, \omega) = -c\delta + \dots$$

with $c = \cos \omega$. In particular $\omega = \mathcal{O}(\delta)$, uniformly in the region (5.32). Hence (5.12) with $s = \sin \omega$ implies claim (5.34). Similarly, (5.13) and $\omega = \mathcal{O}(\delta)$ imply (5.35). Claim (5.36) follows from the uniform expansion (5.35) by the remark preceding the proposition, and the proof is complete. \boxtimes

Lemma 5.4. *Let $0 < \delta \leq \delta_0$ be small enough and consider odd k . Let (Ω_*, ω_*) denote the unique intersection point of the line $\omega = \pi\Omega$ with the 2-scale curve $\Omega = \Omega(\delta, \omega)$. Assume that the hashing line*

$$(5.38) \quad \Omega = \varepsilon(\omega - \pi a_{m, j_m}),$$

of $j_m := [(m+1)/2]$ intersects the line $\pi\Omega = \omega$, $\omega \leq 0$, to the left of (Ω_, ω_*) . Then*

$$(5.39) \quad B_{1,1}^-(\varepsilon) < B_{\min}(\delta) < 0.$$

Proof. We recall $a_{m, j_m} = 1/(2\delta) - 1$; see (5.5). Insertion into hashing (5.38) provides the intersection with $\pi\Omega = \omega$ at

$$(5.40) \quad \begin{aligned} \varepsilon &= \Omega/(\omega - \pi a_{m, j_m}) = \frac{1}{\pi}\Omega/(\Omega - 1/(2\delta) + 1) = \\ &= -\frac{1}{\pi/2}\delta\Omega/(1 - 2\delta - 2\delta\Omega) \geq -\frac{1}{\pi/2}\delta\Omega(\delta, \omega_*)/(1 - 2\delta - 2\delta\Omega(\delta, \omega_*)) \\ &= (\frac{\pi}{2})^{-2}\delta^2/(1 - 2\delta) + \mathcal{O}(\delta^4) = (\frac{\pi}{2})^{-2}(\delta^2 + 2\delta^3 + \mathcal{O}(\delta^4)). \end{aligned}$$

Here we have used intersection to the left of (Ω_*, ω_*) , i.e. $\Omega \leq \Omega_* = \Omega(\delta, \omega_*) < 0$, and expansion (5.34) at (Ω_*, ω_*) . The ε -expansion (4.12) of corollary 4.2 for $B_{1,1}^- = B_{1,1}^-(\varepsilon)$, the estimate $\varepsilon = \varepsilon^- = \mathcal{O}(\delta^2)$ of (5.14), and comparison with (5.40) then yield

$$(5.41) \quad \begin{aligned} B_{1,1}^-(\varepsilon) &= -(\frac{\pi}{2})^2\varepsilon + (\frac{\pi}{2})^3\varepsilon^2 + \mathcal{O}(\varepsilon^3) \leq \\ &\leq -\delta^2 - 2\delta^3 + \mathcal{O}(\delta^4) < B_{\min}(\delta) < 0. \end{aligned}$$

This proves claim (5.39) and the lemma. \boxtimes

6 Proof of theorem 1.2

We summarize the proof of theorem 1.2 as follows. See figs. 2.1 and 2.2 for an illustration. First, let k be odd and large enough, $\varepsilon := 1/\omega_k$, $\omega_k = (k + 1/2)\pi$. In section 2 we have studied the 2-scale characteristic equation (2.7), (2.8) which eliminated $\varepsilon > 0$. Instead, imaginary eigenvalues $\mu = \pm i\tilde{\omega}$ were represented by a slow Hopf frequency $\tilde{\Omega} = \varepsilon\tilde{\omega}$, in addition to $\tilde{\omega}$ itself. The case of real eigenvalues μ , and their crossing at $\mu = 0$ due to the scaled control parameter $b = 2\varepsilon B$, was treated

in lemma 2.1 and corollary 2.2. The hashing $\tilde{\Omega} = \varepsilon\tilde{\omega}$ was detailed, and normalized to $\Omega = \tilde{\Omega} - (2m+1)$, $\omega \equiv \tilde{\omega} \pmod{2\pi}$, in lemma 2.3. In lemma 2.4 we rewrote the characteristic equation in normalized frequencies Ω, ω instead of $\tilde{\Omega}, \tilde{\omega}$. Lemma 2.5 studied the resulting fundamental nonlinear 2-scale relation between Ω and ω . The resulting control parameters B were addressed in lemma 2.6. Emphasis there was on monotonicity properties.

Section 3 was devoted to the resulting nontrivial control-induced Hopf bifurcations, at $B = B_{m,j}^\pm$, in contrast to the spectrum inherited from the uncontrolled case. The detailed analysis included simplicity and the transverse crossing directions; see theorem 3.4. The analysis culminated in corollaries 3.5 and 3.9. In corollary 3.5 we established the absence of any Pyragas control, for control parameters $B > 0$. The central corollary 3.9 established the control region

$$(6.1) \quad B \in \mathcal{P} = (B_{0,1}^+, B_{1,1}^-)$$

as the only Pyragas region, under assumptions (3.77)–(3.79) of certain inequalities among the Hopf parameters $B = B_{m,j}^\pm$.

Section 4 collected ε -expansions for $B_{m,j}^\pm$, and auxiliary quantities like the fast and slow normalized Hopf frequencies $\omega_{m,j}^\pm$ and $\Omega_{m,j}^\pm$, see proposition 4.1. Corollary 4.3 then established the crucial Hopf inequalities (3.77)–(3.79) for small enough $0 < \varepsilon \leq \varepsilon_0(\delta_0)$, uniformly for bounded indices $m \leq m_0$ and $j \leq j_m + 1$ in the Hopf series $B_{m,j}^+$, as well as for $B_{m,j}^-$ with $j \leq j_m$. Here $j_m := [(m+1)/2]$. In particular this settled assumption (3.78). At the end of this section, we observed how our proof hinged on a miraculous gap property of instability intervals $B \in I_{m,j} = (B_{m,j}^-, B_{m,j}^+)$: the first gap occurs at $j = j_m$ and contains the Pyragas region (6.1). See fig. 4.1.

To complete the proof, the limit of large $m > m_0$, alias small $\delta = 1/\Omega_m = 1/(2m+1)$, was addressed in section 5. For odd k , lemma 5.1 collected δ -expansions for $\Omega, B, \varepsilon^\pm$, and $B_{0,1}^+, B_{1,1}^-$ in terms of the (normalized) fast Hopf frequencies ω . In lemma 5.2 this settled the remaining two assumptions (3.77) and (3.79) of corollary 3.9, up to one exceptional case. The exceptional case was caused by our additional assumption, thus far, that all relevant Hopf points $B_{m,j}^-$, $j = 1, \dots, j_m$ in (3.79) occur in the (normalized) frequency range

$$(6.2) \quad -\pi/2 \leq \omega \leq \pi\Omega < 0,$$

i.e. at, or to the right of, the unique intersection (Ω_*, ω_*) of the 2-scale frequency relation (5.6), (2.26), (2.35) with the straight line $\omega = \pi\Omega$ in the (Ω, ω) -plane. Since Hopf points themselves originate from intersections of straight hashing lines with that 2-scale frequency relation, the only remaining case is that the hashing line at $j = j_m = [(m+1)/2]$ intersects $\omega = \pi\Omega$ to the left of (Ω_*, ω_*) . This case was addressed, and settled, in lemma 5.4. Indeed the minimal possible value B_{\min} of control parameters induced by the 2-scale frequency relation then satisfies

$$(6.3) \quad B_{1,1}^-(\varepsilon) < B_{\min}(\delta) < 0.$$

Since $B_{\min} \leq B_{m,j}^-$ for all j , this also established the remaining assumption (3.79) in this one remaining configuration. This completes the proof of our main theorem 1.2.

References

- [BeCo63] R. Bellman and K.L. Cooke. *Differential-Difference Equations*. Academic Press, New York, 1963.
- [Die&al95] O. Diekmann, S.A. van Gils, S.M. Verduyn-Lunel and H.-O. Walther. *Delay Equations: Functional-, Complex-, and Nonlinear Analysis*. App. Math. Sci. **110**, Springer-Verlag, New York, 1995.
- [Dor89] P. Dormayer. Smooth bifurcation of symmetric periodic solutions of functional differential equations. *J. Differ. Equations*. **82** (1989) 109–155.
- [Fie&al07] B. Fiedler, V. Flunkert, M. Georgi, P. Hövel and E. Schöll. Refuting the odd number limitation of time-delayed feedback control. *Phys. Rev. Lett.* **98** (2007) 114101.
- [Fie&al08] B. Fiedler, V. Flunkert, M. Georgi, P. Hövel and E. Schöll. Beyond the odd-number limitation of time-delayed feedback control. In *Handbook of Chaos Control*. (E. Schöll et al., eds.), Wiley-VCH, Weinheim, (2008) 73–84.
- [Fie&al10] B. Fiedler, V. Flunkert, P. Hövel and E. Schöll. Delay stabilization of periodic orbits in coupled oscillator systems. *Phil. Trans. Roy. Soc. A*. **368** (2010) 319–341.
- [FieMP89] B. Fiedler and J. Mallet-Paret. Connections between Morse sets for delay differential equations. *J. Reine Angew. Math.* **397** (1989) 23–41.
- [FiOl16] B. Fiedler and S. Oliva. Delayed feedback control of a delay equation at Hopf bifurcation. *J. Dyn. Differ. Equations*. **28** (2016) 1357–1391.
- [Hale77] J.K. Hale. *Theory of Functional Differential Equations*. Springer-Verlag, New York, 1977.
- [HaleVL93] J.K. Hale and S.M. Verduyn-Lunel. *Introduction to Functional Differential Equations*. Springer-Verlag, New York, 1993.
- [Har&al06] F. Hartung, T. Krisztin, H.-O. Walther and J. Wu. Functional differential equations with state-dependent delays: theory and applications. In *Handbook of Differential Equations: Ordinary Differential Equations, Vol. III*. (A. Cañada, P. Drábek and A. Fonda eds.), Elsevier/North-Holland, Amsterdam, (2006) 435–545.
- [Ju&al07] W. Just, B. Fiedler, V. Flunkert, M. Georgi, P. Hövel and E. Schöll. Beyond the odd number limitation: A bifurcation analysis of time-delayed feedback control. *Phys. Rev. E*. **76** (2007) 026210.
- [KapYor74] J.L. Kaplan and J.A. Yorke. Ordinary differential equations which yield periodic solutions of differential delay equations. *J. Math. Analysis Appl.* **48** (1974) 317–324.
- [KolMysh99] V. Kolmanovskii and A. Myshkis. *Introduction to the Theory and Applications of Functional Differential Equations*. Kluwer, Dordrecht, 1999.
- [Kri08] T. Krisztin. Global dynamics of delay differential equations. *Period. Math. Hung.* **56** (2008) 83–95.

- [Kur71] J. Kurzweil. Small delays don't matter. In *Proc. Symp. Differential Equations and Dynamical Systems*, Warwick 1969 (D. Chillingworth ed.), Springer-Verlag Berlin 1971, 47–49.
- [Lop17] A. López Nieto. Heteroclinic connections in delay equations. Master's Thesis, Freie Universität Berlin, 2017.
- [MP88] J. Mallet-Paret. Morse decompositions for differential delay equations. *J. Differ. Equations*. **72** (1988) 270–315.
- [MPNu92] J. Mallet-Paret and R.D. Nussbaum. Boundary layer phenomena for differential-delay equations with state-dependent time-lags: I. *Arch. Ration. Mech. Analysis* **120** (1992) 99–146.
- [MPNu96] J. Mallet-Paret and R.D. Nussbaum. Boundary layer phenomena for differential-delay equations with state-dependent time-lags: II. *J. Reine Angew. Math.* **477** (1996) 129–197.
- [MPNu03] J. Mallet-Paret and R.D. Nussbaum. Boundary layer phenomena for differential-delay equations with state-dependent time-lags: III. *J. Differ. Equations* **189** (2003) 640–692.
- [MPNu11] J. Mallet-Paret and R.D. Nussbaum. Stability of periodic solutions of state-dependent delay-differential equations. *J. Differ. Equations*. **250** (2011) 4085–4103.
- [MPSe96a] J. Mallet-Paret and G. Sell. Systems of differential delay equations: Floquet multipliers and discrete Lyapunov functions. *J. Differ. Equations* **125** (1996) 385–440.
- [MPSe96b] J. Mallet-Paret and G. Sell. The Poincaré–Bendixson theorem for monotone cyclic feedback systems with delay. *J. Differ. Equations* **125** (1996) 441–489.
- [Nu78] R.G. Nussbaum. *Differential-Delay Equations with Two Time Lags*. Mem. Am. Math. Soc. **205**, Providence, RI, 1978.
- [Nu02] R.G. Nussbaum. Functional differential equations. In *Handbook of Dynamical Systems, Vol. II*. (B. Fiedler ed.), Elsevier/North-Holland, Amsterdam, (2002) 461–499.
- [Nak97] H. Nakajima. On analytical properties of delayed feedback control of chaos. *Phys. Lett. A*. **232** (1997) 207–210.
- [NakUe98] H. Nakajima and Y. Ueda. Half-period delayed feedback control for dynamical systems with symmetries. *Phys. Rev. E*. **58** (1998) 1757–1763.
- [Pyr92] K. Pyragas. Continuous control of chaos by self-controlling feedback. *Phys. Lett. A*. **170** (1992) 421–428.
- [Pyr12] K. Pyragas. A twenty-year review of time-delay feedback control and recent developments. *Int. Symp. Nonl. Th. Appl.*, Palma de Mallorca, 2012.
- [Wal95] H.-O. Walther. *The 2-Dimensional Attractor of $\dot{x}(t) = -\mu x(t) + f(x(t-1))$* . Mem. Amer. Math. Soc. **544**, Providence, RI, 1995.

- [Wri55] E.M. Wright. On a non-linear differential-difference equation. *J. Reine Angew. Math.* **194** (1955) 66–87.
- [Wu96] J. Wu. *Theory and Applications of Partial Functional Differential Equations*. Springer-Verlag, New York, 1996.
- [YuGuo14] J. Yu and Z. Guo. A survey on the periodic solutions to Kaplan-Yorke type delay differential equation-I. *Ann. Differ. Equations.* **30** (2014) 97–114.